Queen's University Belfast
School of Chemistry and Chemical Engineering

Chemical Engineering

Master Thesis

Phosphate adsorption onto laterite and laterite waste from a leaching process

Martín Méndez Pasarín

Supervisors: Dr. Gavin M. Walker; Prof. Stephen J. Allen

Submission date: 26/03/2012

Queen's University Belfast

Abstract

It has been proved by several authors that adsorption is a good way to remove phosphate from wastewaters, especially using fly ash or modified fly ash as an adsorbent. There are also various studies regarding removal of arsenic and mercury with an adsorbent called laterite, which is a type of soil rich in iron and aluminium, usually formed in hot and wet tropical areas.

The main aim of this research is to study the removal capacity of laterite and modified laterite toward phosphate. Different kinds of laterite have been provided by Kinney Environmental Science Services Consultancy, a local company based in Northern Ireland. Properties of laterite have been determined using X-ray diffractograms.

One of the innovations presented in this thesis is the calibration of phosphorus with a colorimetric method. It was carried out in order to avoid the use of much more expensive methods, such as the Inductively Coupled Plasma spectrometry (ICP). Subsequent adsorption experiments include: adsorption kinetics, pH studies, adsorption isotherms, temperature studies, thermodynamic parameters and column studies. Laterite charred at different temperatures has been used and different particle sizes have also been tested.

Finally, a global comparison of the results with other authors has been made, as well as with some other synthesized materials that could be used for future research.

Acknowledgments

Writing this master thesis would not have been possible without the support of several mentors. First of all I would like to thank Dr. Tony McNally for giving me the opportunity to carry out all the experiments and write this thesis at the School of Chemistry and Chemical Engineering within the Queen's University of Belfast. Special thanks go to my supervisor Dr. Gavin M. Walker and PhD student Yoann Glocheux for their great support to my thesis, as well as John Kinney from KESS-Consult for providing the adsorbent I have been using for these last months. Further, I would like to show my gratitude to all the members of the Adsorption Group for their friendliness towards me.

I would also like to thank all the friends that I have made during this unforgettable Erasmus exchange. Special thanks go to Irina Díaz, Philipp Neumann, Stefan Taalman, Annabelle Perret, Mathilde Felber, Ciaran Doherty, Jenny McAfee, Adam Downey, Adam Young, Paul Walsh, Íñigo Blond, Marco Ciavola, Dora Scapin and Guillermo Llorente for standing and supporting me, as well as for all the experiences that we have shared in Belfast.

My deep gratitude goes to my parents José and Delfina, for the opportunity to study and their support during my student's career. Finally, I would like to thank my friends and family from Spain for their remarkable support throughout these past five years of my degree, these include Carlos Fernández, Marta Sànchez, Alejandro Marín, Cristina Casal, David Sáiz, Daniel Galeano, Pedro J. Aguas, Marc Dalmau, Daniel García, Arnau Mestres, Eduard Laguarda, Mª Carmen Balsalobre, David Gracia, Mariona Vilà, Montserrat Soro, Alberto Díaz, Sonia Miranda and Elena Rois, amongst others.

Table of Contents

1. Introduction

Phosphorus is one of the more common elements on earth and is essential to all living organisms. It is found combined with other elements in the earth's crust in the form of phosphate rock. The major commercial deposits are in the United States, China, the former Soviet Union, Morocco, Finland, South Africa, and some Pacific Islands. It is estimated that there are 40 billion tons of reserves of phosphate rock or a 250-year supply at current usage. This may seem like an abundant supply, but some of this material is not accessible or of poor quality. In addition, we are using this material at an increasing rate. In fact, phosphate is recognised as being one of the resources that will be lost in near future.

Figure 1. Different kinds of phosphorus: waxy white, red and violet phosphorus.

A large amount of used phosphate finally reaches water environment as diluted waste, which often leads to pollution of the water environment. It is of value to collect the finally disposed phosphates from effluents and drain water before further dispersion and dilution of them in the water environment.

Phosphorus is often regarded as the main culprit in cases of eutrophication in lakes. Eutrophication is the term used to describe the process of nutrient enrichment, where a water body gradually changes from a nutrient poor state (oligotrophic) to a nutrient rich state (eutrophic). It is defined in the European Commission's Urban Waste Water Treatment (EC UWWT) Directive (91/271/EEC) as:

"The enrichment of water by nutrients, especially compounds of nitrogen and/or phosphorus, causing accelerated growth of algae and higher forms of plant life to produce an undesirable disturbance to the balance of organisms present in the water and to the quality of water concerned."

The concentration of algae and the trophic state of lakes correspond well to phosphorus levels in water. Studies conducted in the Experimental Lakes Area in Ontario (Canada) have shown a relationship between the addition of phosphorus and the rate of eutrophication.

Figure 2. Eutrophication from phosphorus contamination. Source: US EPA.

In 2005, The Environmental Protection Agency identified eutrophication as the major threat to water quality in Ireland, with the basic cause in most cases likely to be excess phosphorus inputs. Eutrophication also poses the most widespread single threat to good water quality in Northern Ireland while in the United Kingdom 23% of lakes are considered to be eutrophic. Freshwater lakes are considered to be eutrophic if the phosphorus concentration exceeds 35 g P L^{-1}; by this standard both Lough Neagh and Lough Erne from Northern Ireland can be considered to be highly eutrophic. Phosphate removal from wastewaters is important for the control of eutrophication and is enforced by increasingly stringent legislation e.g. the European Urban Wastewater Treatment Directive 91/271 and 98/15.

Many techniques have been proposed for the removal of phosphate from wastewater. Coagulation–precipitation and biological methods are widely accepted methods of phosphate removal at industrial level. Extensive research has also been carried out to produce simplification of maintenance, stable running and removal efficiency. Among these researches, many researchers have promoted development of adsorbents with high selectivity and removal capacity for phosphate. Furthermore, adsorption is known more useful and economical. In this project, this technique is proposed as a possible solution for phosphate removal using local laterite –a kind of mineral rich in iron and aluminium– as an adsorbent.

2. Adsorption of Phosphates

2.1. Background and Literature Review

Adsorption involves, in general, the accumulation (or depletion) of solute molecules at an interface (including gas-liquid interfaces, as in foam fractionation, and liquid-liquid interfaces, as in detergency). In this project only liquid-solid interfaces are considered, with solute distributed selectively between the fluid and solid phases. Adsorption separation has been widely used in environmental chemistry, owing to its relatively low cost, simplicity of design and operation, and pollutant removal to low concentrations. Among the possible separation and purification techniques, adsorption by selective adsorbent shows promise in being among the most attractive and efficient methods for purification and separation of trace anion contaminants.

Adsorbents are natural or synthetic materials of amorphous or microcrystalline structure. Those used on a large scale, in order of sales volume, are activated carbon, molecular sieves, silica gel, and activated alumina, amongst others.

Figure 3. Activated carbon. Source: Calgon Carbon.

Regarding phosphates removal, several studies have been done using both chemical and biological methods, which have traditionally been proposed for phosphate removal from water and wastewater. Coagulation and biological methods are used in industries but these treatment processes are unable to satisfy the mandate level or reduce it to near zero or below 10 mg/L (Stante et al., 1997; Zhao and SenGupta, 1998; Bektas et al., 2004; Vasudevan et al., 2008; Namasivayam and Prathap, 2005; Babatunde et al., 2008; Yildiz, 2004; de-Bashan and Bashan, 2004). Therefore, extensive researches have been investigated to develop suitable methods based on stable running, simple operation technique, high selectivity and excellent kinetic performances. Ion exchange adsorbents, electrodialysis, and specially ligand exchangers possess all of these characteristics.

Fly ash is a very common adsorbent used for phosphate adsorption; several studies have been made using both fly ash and modified fly ash with particularly good results in this last case due to the increase of the specific surface area of the fly ash (Lu et al., 2009; Xu et al., 2010). In some cases, the phosphate removal percentage reached percentages between 90-97%, although the total removal was mainly through precipitation, with a relative contribution of adsorption to the total removal accounting for 30-34%.

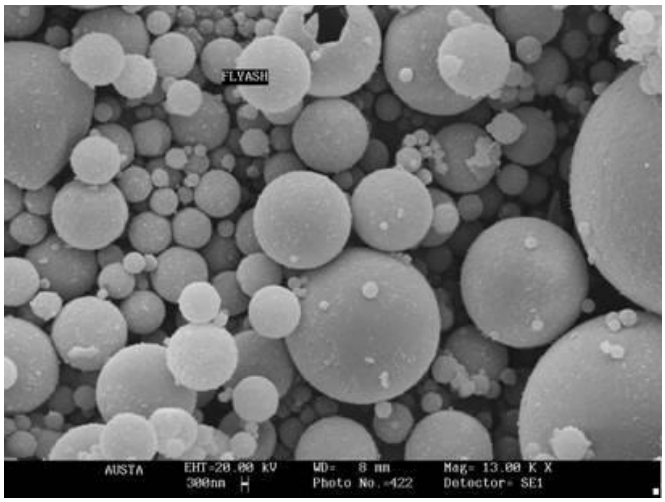

Figure 4. Micrograph of fly ash particles taken using a Scanning Electron Microscope (SEM). Source: Fly Ash Australia.

Other minor studies about adsorptive removal of phosphate have been done with numerous kinds of adsorbents, such as peat (Xiong and Mahmood, 2010), red mud (Chang-jun et al., 2007), iron oxide tailings (Zeng et at., 2004), vesuvianite (Li et al., 2009), skin split waste (Huang et al., 2009), calcite (Karageorgiou et al., 2007), or alunite (Özacar, 2003).

Laterite has also traditionally been used in adsorption, and its properties regarding arsenic and mercury are widely well-known (Yu et al., 2008; Maji et al., 2007, Partey et al., 2008). It has been proved that about 98% arsenite can be removed using a laterite dose of 40 g/L, for an initial arsenite concentration of 1 mg/L (Maiti et al., 2010).

Nevertheless, only a few studies have used laterite for phosphate removal. Some temperature studies undertaken by Zhang et al., (2010) are worth noting, as they showed that the capacity of the laterite for phosphorus adsorption increases with temperature. In Northern Ireland, a research project was carried out in the University of Ulster regarding the use of local laterite in phosphorus and heavy metal removal (Wood and McAtamney, 1996). In this study, a pilot-scale experimental constructed wetland containing laterite achieved up to a 96% removal of phosphorus.

2.2. Phosphorus Regulations in Northern Ireland

Under the Northern Ireland Water Act 1972, the Environment and Heritage Service (EHS), an Executive Agency within the Department of the Environment for Northern Ireland, has a duty to promote the conservation of water resources of Northern Ireland (NI) and the cleanliness of water in waterways and underground strata. Eutrophication is considered by EHS to pose the most widespread single threat to good water quality in Northern Ireland.

The most widely used classification of lake trophic status is that proposed by the Organisation for Economic Co-operation and Development (OECD) and described in Table 1. Lakes are classified in terms of the average phosphorus concentration, the average and maximum crops of algae (estimated by the pigment chlorophyll *a*) and the measurement of water transparency. The OECD scheme proposed three main classes: oligotrophic for nutrient poor waters, mesotrophic for waters slightly to moderately enriched with nutrients. In addition two boundary classes were proposed: ultra-oligotrophic for extremely nutrient and alegal concentrations. The accompanying table shows the range of values proposed for each of these classes. The relevant data for Lough Neagh, Lower Lough Erne and Upper Lough Erne are also presented in Table 1. It is clear that each lake is eutrophic and, in fact, both Lough Neagh and Upper Lough Erne generally fall into the hypertrophic class.

Table 1. OECD lake trophic classification criteria for phosphorus. Source: EHS.

	Total Phosphorus Mean $\mu g\ Pl^{-1}$	Chlorophyll *a*		Transparency Secchi disc depth	
		Mean $\mu g\ Pl^{-1}$	Maximum $\mu g\ Pl^{-1}$	Mean m	Minimum m
Ultra-oligotrophic	<4	<1.0	<2.5	>12	>6
Oligotrophic	<10	<2.5	<8	>6	>3
Mesotrophic	10-35	2.5-8.0	8.25	6-3	3-1.5
Eutrophic	35-100	8.25	25-75	3-1.5	1.5-0.7
Hypereutrophic	>100	>25	>75	<1.5	<0.7
Lough Neagh#	165	67	144	1.1	0.6
Lower Lough Erne#	64	9	60	2.1	1.6
Upper Lough Erne#	87	31	101	N/A	N/A

But eutrophication has also affected Northern Irish rivers. The rivers in NI are classified under the General Quality Assessment (GQA) systems using routine chemical and macroinvertebrate biological monitoring. The chemical quality classification does not require measurement of phosphorus, and classifying rivers in terms of their trophic status using phosphorus concentrations remains questionable. The criteria for identification of Sensitive Areas under the EC UWWT Directive suggest that a river is excessively enriched if the mean concentration for soluble phosphates is greater than 100 µg P L^{-1}.

The biological GQA classification system is based on the presence of various macroinvertebrate species, which are sensitive to a range of pollutants. From 1994 to 1997 this biological monitoring programme was complemented by surveys of macrophytes in NI rivers. The presence and abundance of macrophytes provide an index of environmental disturbance due to nutrient enrichment and the surveys showed that most rivers in NI are enriched. The level of enrichment in the Lagan, Foyle and Blackwater catchments was sufficiently severe for plant respiration to reduce dissolved oxygen levels in rivers. These findings were the first reliable indication that eutrophication is a significant problem in a number of river catchments in NI.

Continuing studies on nutrient enrichment of lakes in NI have included the collection of data on soluble phosphate for rivers flowing into Lough Neagh and Lough Erne along with data for the River Bush. The average phosphate concentrations for these rivers measured during 1997 are summarised in Figure 5 and indicate that many rivers currently exceed the EC UWWT Directive 100 µg P L^{-1} criteria highlighted above.

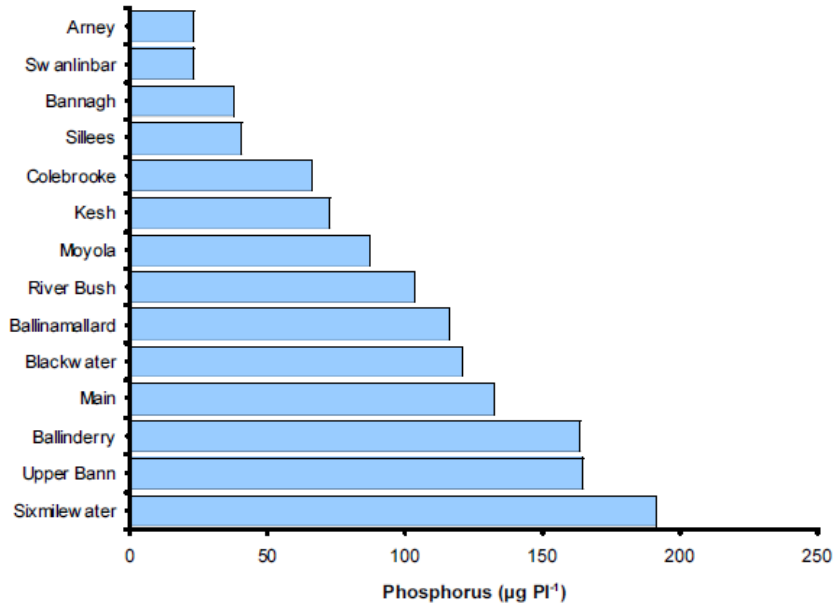

Figure 5. Phosphate concentrations in NI rivers. Source: EHS.

As regards phosphate contamination caused by agriculture, on January 1st, 2007, new legislation came into operation in Northern Ireland introducing measures to improve the use of nitrogen and phosphorus nutrients on farms. Its aim is to improve water quality by protecting water against pollution caused by nitrates from agricultural sources. It stipulates, among other things, that organic manures including dirty water must not be applied within:

- 20 m of lakes;
- 50 m of a borehole, spring or well;
- 250 m of a borehole used for a public water supply;
- 15 m of exposed cavernous or karstified limestone features;
- 10 m of a waterway other than lakes; this distance may be reduced to 3 m where slope is less than 10% towards the waterway and where organic manures are spread by bandspreaders, trailing shoe, trailing hose or soil injection or where adjoining area is less than 1 ha in size or not more than 50 m in width.

Furthermore, one of the factors to be considered if planning to spread fertilizer on sleepy sloping land is the proximity of waterway. The distance from the area where spreading is planned to the nearest waterway at the bottom of the slope should be assessed. For organic manures, high risk is defined as less than 20 m from a waterway other than a lake, moderate risk is 20-30 m and low risk is more than 30 m. In the case of lakes, for organic manures, high risk is defined as less than 30 m from a lake, moderate risk is 30-40 m and low risk is more than 40 m. For chemical fertilisers, high risk is less than 5 m from any waterway, moderate risk is 5-10 m and low risk is more than 10 m.

3. Materials and Methods

3.1. Chemicals and Adsorbents

- Deionized distilled water was used to prepare all solutions and suspensions.
- Standard solution of phosphorus (P) 1000 + 2 µg/mL –provided by JVA Analytical– was used to obtain the different dilutions of the calibration curve explained in section 5 (Phosphate calibration).
- Aqueous solutions of ascorbic acid ($C_6H_8O_6$) were prepared according to Lenoble et al. The concentration of ascorbic acid in the stock solution was 0.57 mol/L (10.03 g of solid ascorbic acid in 100 mL of deionized water).
- The molybdate stock solution was prepared by dissolution of 5.2 g ammonium molybdate and 8.8 mg of potassium antimonyl tartrate in 30 ml of 9 mol/L sulfuric acid (H_2SO_4) and diluted by deionized water to a final volume of 50 ml in a volumetric flask. (Tsang et al., 2006).

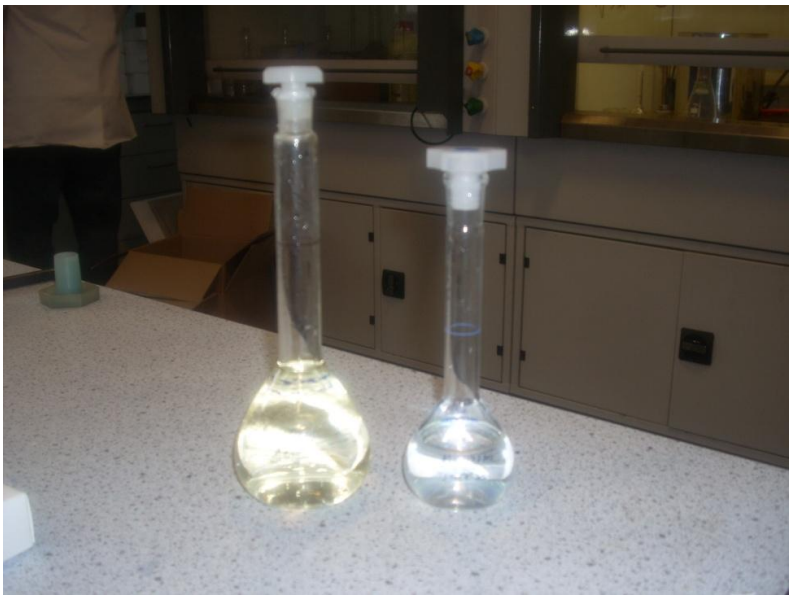

Figure 6. Ascorbic acid (yellow) and molybdate stock solution (white).

- The rest of phosphate solutions were prepared by dilutions of a synthetic phosphorus solution comprising deionized water and a certain amount of an 85% calcium dihydrogen phosphate ($Ca(H_2PO_4)_2$) salt, according to the stoichiometry of the following reaction:

$$Ca\left(H_2PO_4\right)_2 \rightarrow Ca^{2+} + 2\ H_2PO_4^-$$

- Sodium hydrogen carbonate ($NaHCO_3$) was used as a pH buffer in most of the experiments.
- Different solutions of hydrochloric acid (HCl) and sodium hydroxide (NaOH) within a range from 0.1 mM to 0.1 M were used to adjust the pH of the phosphate solution when necessary.
- Three different kinds of laterite were provided by Kinney Environmental Science Services Consultancy (KESS-Consult, Co. Antrim, Northern Ireland). Two of them were from different layers: an upper layer (sample called “upper”) and a lower layer (sample called “lower”). Additionally, a waste resulting from a H_2SO_4 leaching on laterite was also included (sample called “acidified”).

Figure 7. Samples “upper”, “lower” and “acidified” from the provided laterite.

The three kinds of laterite were subsequently cleaned, dried and sieved until the following granule size distribution was obtained:

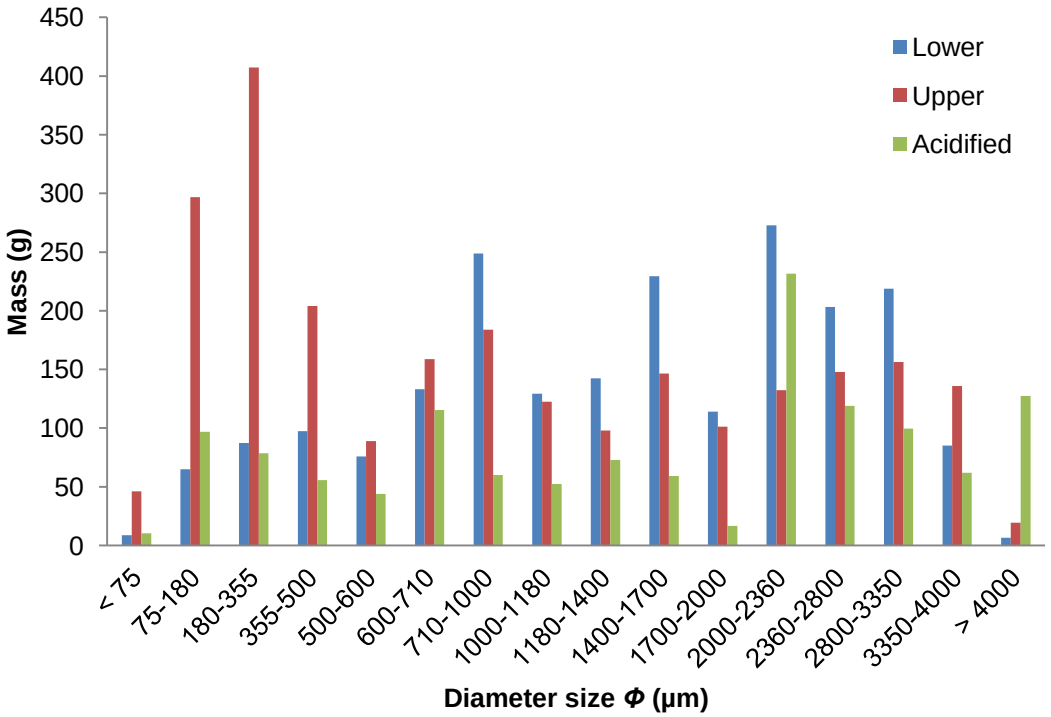

Figure 8. Granulometric distribution of the three kinds of laterite.

3.2. Adsorption Kinetics

The batch experimental data from this study will be applied to selected adsorption kinetic models, namely pseudo-first-order and pseudo-second-order models.

The form of the pseudo-first-order (or Lagergren first-order) rate equation is as follows:

$$\frac{dq}{dt} = k_1(q_e - q_t) \tag{1}$$

Where:

- q_e is the equilibrium adsorption of phosphorus adsorbed on unit mass of the laterite (mg/g), and can be calculated by using the following expression:

$$q_e = \frac{(C_0 - C_e)V}{m} \tag{2}$$

  where C_0 and C_e are the initial phosphorus concentration (mg/L) and phosphorus concentration (mg/L) at equilibrium respectively; V is the volume of the phosphorus solution (L); and m is the weight of laterite used (g).

- q_t is the amount of adsorbate adsorbed (mg/g) at time t, defined as:

$$q_t = \frac{(C_0 - C_t)V}{m} \tag{3}$$

  where C_t is the phosphorus concentration (mg/L) at time t.

- k_1 is the pseudo-first-order adsorption rate constant (h^{-1}).

After integration and applying boundary conditions $t = 0$ to $t = t$ and $q_t = 0$ to $q_t = q_t$, the integrated form of equation (1) becomes:

$$\ln(q_e - q_t) = \ln q_e - k_1 t \tag{4}$$

The values of k_1 and q_e can be calculated from the intercept and slope of the plots of $\ln(q_e - q_t)$ versus t.

The pseudo-second-order equation is also based on the sorption capacity of the solid phase and is expressed as:

$$\frac{dq}{dt} = k_2(q_e - q_t)^2 \tag{5}$$

Where:

- k_2 is the rate constant of second-order adsorption (g mg^{-1} h^{-1}).

For the same boundary conditions, the integrated form of equation (5) becomes:

$$\frac{t}{q_t} = \frac{1}{k_2 q_e^2} + \left(\frac{1}{q_e}\right) t \tag{6}$$

If second order kinetics is applicable, then the plot of t/q against t should give a linear relationship, from which q_e and k_2 can be determined from the slope and intercept of plot respectively.

3.3. Freundlich and Langmuir Isotherms

There are basically two well established types of adsorption isotherm: the Freundlich adsorption isotherm and the Langmuir adsorption isotherm.

The Freundlich model is often expressed as:

$$q_e = K_F C_e^{1/n} \tag{7}$$

where K_F and n are constants related to adsorption capacity and energy of adsorption.

The previous equation can be linearized as:

$$\ln q_e = \ln K_F + \left(\frac{1}{n}\right) \ln C_e \tag{8}$$

Therefore, the two Freundlich constants can be easily determined from the plot of ln q_e versus ln C_e.

The Langmuir equation has the following expression when applied to P sorption:

$$q_e = \frac{K_L Q_0 C_e}{1 + K_L C_e} \tag{9}$$

Or, alternatively:

$$\frac{C_e}{q_e} = \frac{1}{K_L Q_0} + \frac{1}{Q_0} C_e \tag{10}$$

Where:

- K_L is a constant related to the binding strength of phosphate (L/mg).
- Q_0 is the Langmuir sorption maximum (mg/g).

These two parameters can be calculated from the linearized Langmuir model, through the slope and the intercept of the plot of C_e/q_e in front of C_e.

3.4. Thermodynamic Parameters

The thermodynamic parameters, namely the standard Gibbs free energy (ΔG^0), change in enthalpy (ΔH^0) and entropy change (ΔS^0) are estimated as follows. The change in Gibbs free energy of the process is related to equilibrium constant by the following equation:

$$\Delta G^0 = -RT \ln K_0 \tag{11}$$

Where:

- K_0 is the equilibrium constant, which can be calculated as:

$$K_0 = \frac{q_e}{C_e} \tag{12}$$

- R is the ideal gas constant (8.314 J mol^{-1} K^{-1}).
- T is the absolute temperature (K).

Gibbs free energy change is also related to the enthalpy change (ΔH^0), and entropy change (ΔS^0) at constant temperature by the following expression:

$$\Delta G^0 = \Delta H^0 - T\Delta S^0 \tag{13}$$

Combining equations (10) and (12) gives the integrated form of the van't Hoff equation:

$$\ln K_0 = \frac{\Delta S^0}{R} - \frac{\Delta H^0}{RT} \tag{14}$$

Therefore, the values of entropy change (ΔS^0) and enthalpy change (ΔS^0) can be obtained from intercept and slope of the plot of $\ln K_0$ versus ($1/T$). Subsequently, the value of Gibbs free energy (ΔG^0) can be calculated from either equation (11) or (13).

4. Experimental Results and Discussion

4.1. Properties of Laterite

The solid structure of the three kinds of laterite was analyzed using X-ray fluorescence (XRF). The result of this analysis is shown in Table 2, giving the main chemical composition of samples.

Table 2. Main chemical compositions of laterite.

Composition (%)	Upper	Lower	Acidified
SiO_2	9.96	27.54	35.33
TiO_2	4.22	4.05	4.48
Al_2O_3	56.55	33.29	33.80
Fe_2O_3	26.20	31.97	23.06
Mn_3O_4	0.20	0.23	0.14
MgO	1.19	0.92	1.00
CaO	0.80	0.60	0.74
Na_2O	0.16	0.12	0.33
K_2O	0.01	0.03	0.15
P_2O_5	0.25	0.23	0.15
SO_3	0.09	0.07	0.07
V_2O_5	0.12	0.13	0.09
Cr_2O_3	0.08	0.11	0.06
SrO	0.02	0.02	0.02
ZrO_2	0.08	0.09	0.07
BaO	< 0.006	< 0.007	< 0.006
NiO	0	0.04	0.01
CuO	0.01	0.02	0.01
ZnO	0.01	0.02	0.01
PbO	0.02	0.02	0.02
HfO_2	0.01	< 0.005	< 0.004
Loss of ignition	22.94	13.52	15.29
Total	99.97	99.49	99.54

Some other properties were also studied, as shown in Table 3 below:

Table 3. Main properties of laterite.

Property	Upper	Lower	Acidified
Point of zero charge (pH_{pzc})	7.8	8.0	5.2
BET surface area (m^2/g)			
Φ < 75 µm	24.79	50.61	85.70
500 µm < Φ < 600 µm	30.13	55.59	98.48
1 mm < Φ < 1.18 mm	29.90	50.79	99.36
Mean pore size (nm)			
Φ < 75 µm	6.74	6.36	4.27
500 µm < Φ < 600 µm	7.28	6.22	4.22
1 mm < Φ < 1.18 mm	6.98	6.30	4.27
Porosity (cm^3/g)			
Φ < 75 µm	0.08	0.16	0.18
500 µm < Φ < 600 µm	0.11	0.17	0.21
1 mm < Φ < 1.18 mm	0.10	0.16	0.21

Finally, various Secondary Electron Images (SEI) were obtained –see Figure 9 below– in order to understand the intern shape of the particles of laterite.

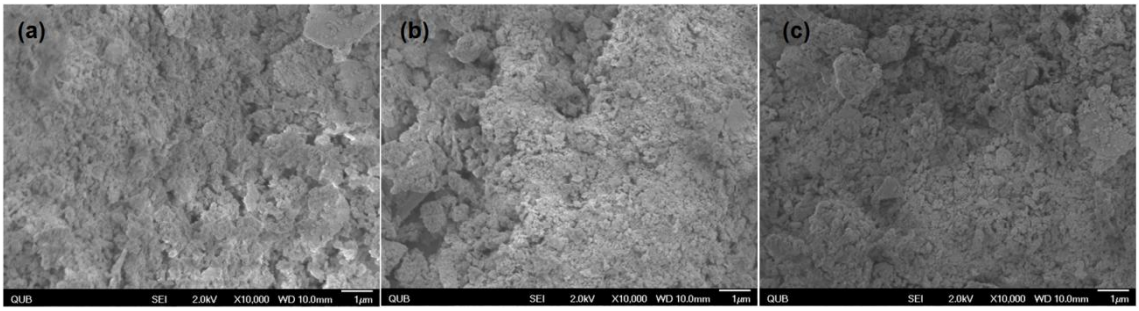

Figure 9. SEM Images of laterite particles: (a) Lower; (b) Upper; (c) Acidified.

From the figure above it is clear that the adsorbent surface has a highly porous structure with heterogeneous structure, especially in the sample with “acidified” laterite.

4.2. Phosphate Calibration

4.2.1. Colorimetric Method

According to S. Tsang et al., the optimized procedure for the determination of phosphate over the 0-5 µmol/L range is described below:

a) 9.3 mL of analyte solution is measured out in a 10 mL volumetric flask;
b) Add 0.1 mL of 98% H_2SO_4, shake;
c) Wait 45 s and add 0.4 mL of molybdate stock solution; shake;
d) Wait 45 s and add 0.2 mL of ascorbic acid stock solution; shake;
e) Wait approximately 10 minutes and then measure absorbance at a single wavelength λ = 880 nm.

In order to apply this procedure to the phosphates calibration, various dilutions of a 10 ppm (mg/L) phosphorus standard solution were prepared, along with a blank of deionized water. Subsequently, the absorbance was read with a DR 2800 Spectrophotometer.

Figure 10. Hach DR 2800TM Portable Spectrophotometer.

The results of the experimental procedure are shown in Table 4 below:

Table 4. Results of the absorbance read for the phosphate dilutions.

***C* (ppm)**	1.0	1.5	2.0	2.5	3.0	4.0	5.0
***A* (AU)**	0.442	0.548	0.663	0.773	0.891	1.107	1.403

4.2.2. Calibration Curve

The concentration dependence of the absorbance was graphically represented in order to obtain a correlation between both magnitudes, as seen in Figure 11 below:

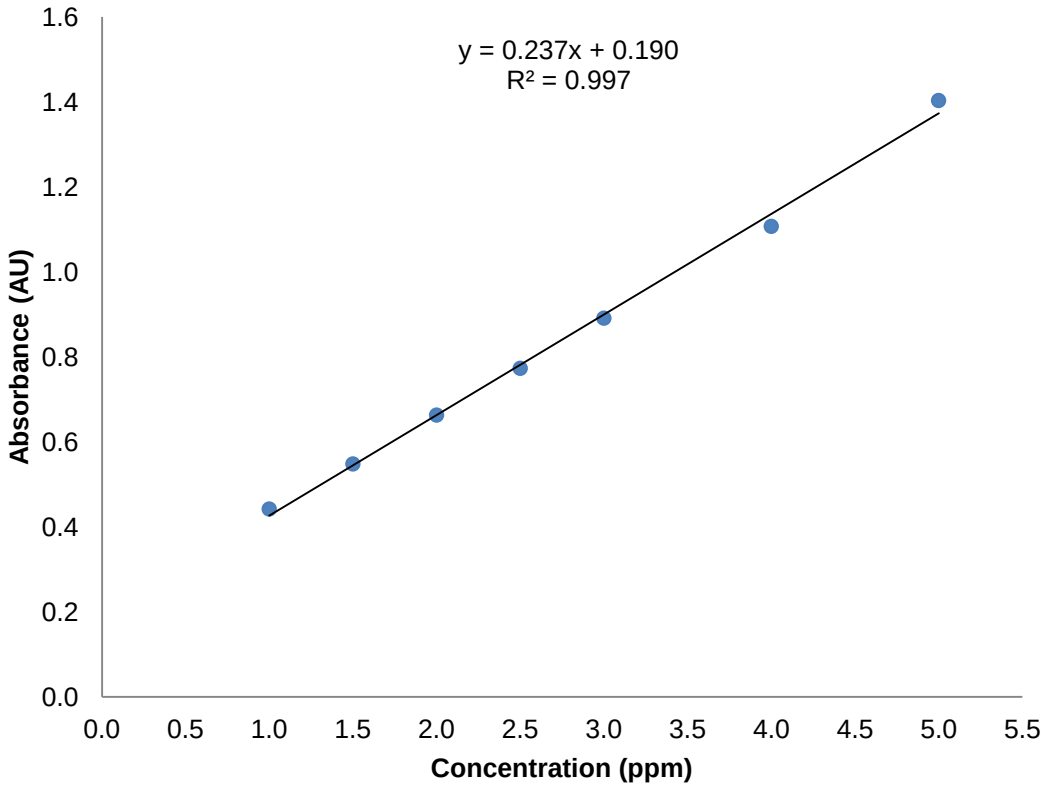

Figure 11. Phosphorus calibration curve within the range from 1 to 5 ppm.

According to the above graph, the mathematical model that gives the relation between the absorbance (*A*) and the concentration of phosphorus (*C*) for the range from 1 to 5 ppm is given as follows:

$$A = 0{,}237\,C + 0{,}190 \tag{15}$$

This equation was used from now then to determinate the concentration of phosphorus in all the subsequent experiments and studies. Its validity was also studied by measuring the absorbance of a 2.5 ppm phosphorus solution made from a $Ca(H_2PO_4)_2$ salt, which gave a relative error between the calculated concentration and the original concentration of 5.86%, which is pretty acceptable if we consider its economic advantages in comparison with another methods, such as the Inductively Coupled Plasma spectrometry (ICP).

4.3. Adsorption Kinetics

4.3.1. Preliminary Study

Some preliminary studies were done to estimate how long it takes for the adsorption process to reach equilibrium, and also to see the effect of the kind of layer and the particle size. These experiments were made under the following conditions:

- Temperature: T = 25 ºC (Room temperature).
- Initial concentration of phosphorus [P]: C_0 = 50 ppm.
- Volume of the flasks: V = 200 mL.
- Mass of adsorbent (laterite): m = 0.2 g (Dose = 1 g/L).
- Mass of pH buffer ($NaHCO_3$): 20 mg (Dose = 100 mg/L).
- Initial pH: 7.0 (constant due to the pH buffer).
- Stirrer speed: 500 rpm (RCT basic IKAMAG® safety control).

Figure 12. RCT basic IKAMAG® safety control magnetic stirrer.

- Volume of the samples: 10 mL.
- The samples were taken at the intervals of 0, 2, 6, 24, 48 hours after the start of the adsorption reaction, and subsequently diluted and analyzed in the spectrophotometer after following the procedure of the colorimetric method.
- For each one of the intervals, the concentration of phosphorus was calculated with equation (15) and later re-calculated considering the dilution factor in order to obtain the real concentration.

This procedure was followed for three different experiments: the first one using the layer of laterite called “lower”, the second one with the layer called “upper”, and the third one with the layer called “acidified”.

In each case, three different particle sizes (in function of the diameter Φ) were also used: Φ < 75 µm; 500 µm < Φ < 600 µm; and 1 mm < Φ < 1.18 mm.

The results from the experiments are outlined in Figures 13, 14 and 15:

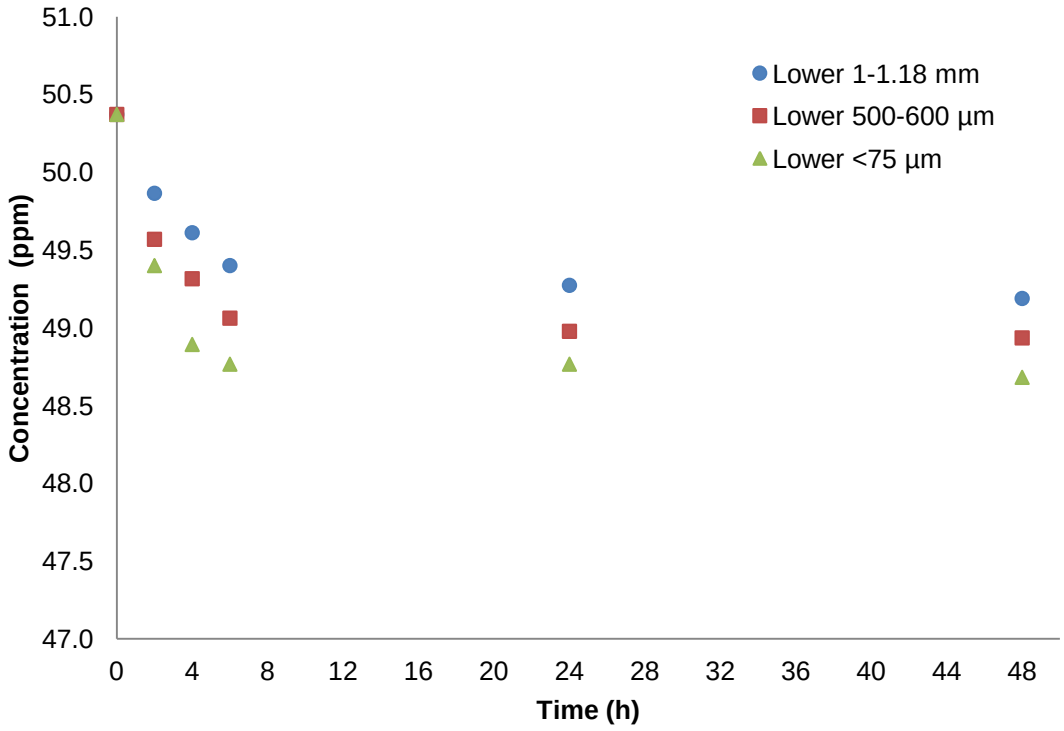

Figure 13. Kinetics of phosphorus sorption on “lower” laterite for particle sizes: Φ < 75 µm; 500 µm < Φ < 600 µm; and 1 mm < Φ < 1.18 mm.

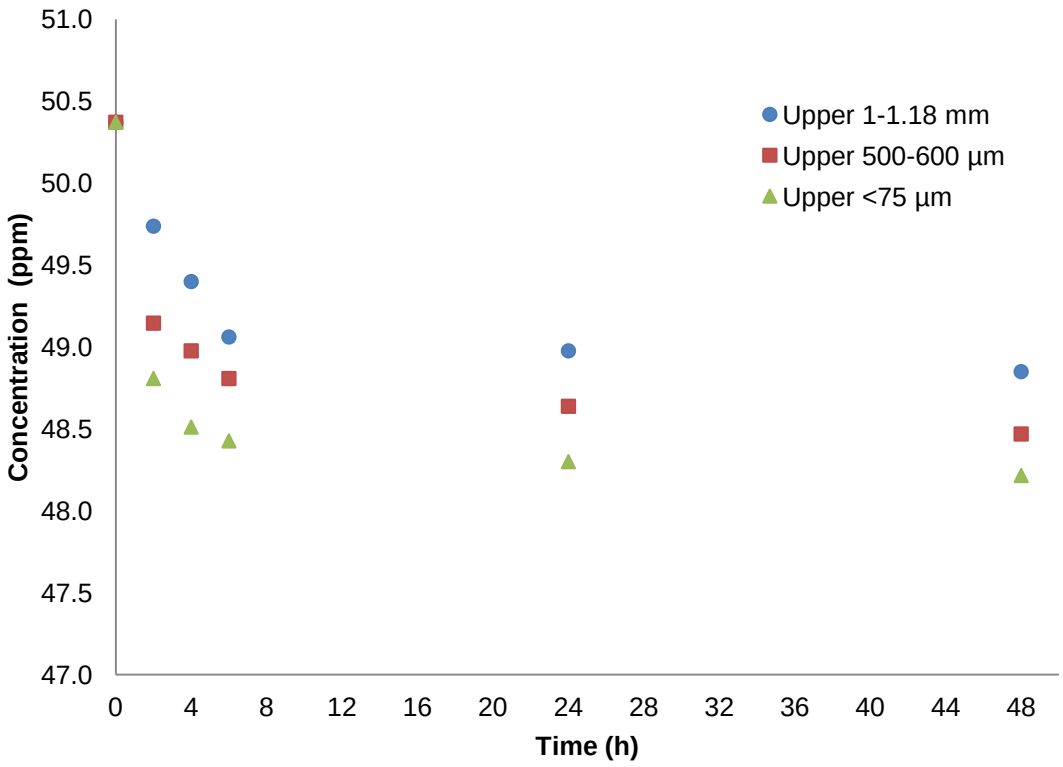

Figure 14. Kinetics of phosphorus sorption on “upper” laterite for particle sizes: Φ < 75 µm; 500 µm < Φ < 600 µm; and 1 mm < Φ < 1.18 mm.

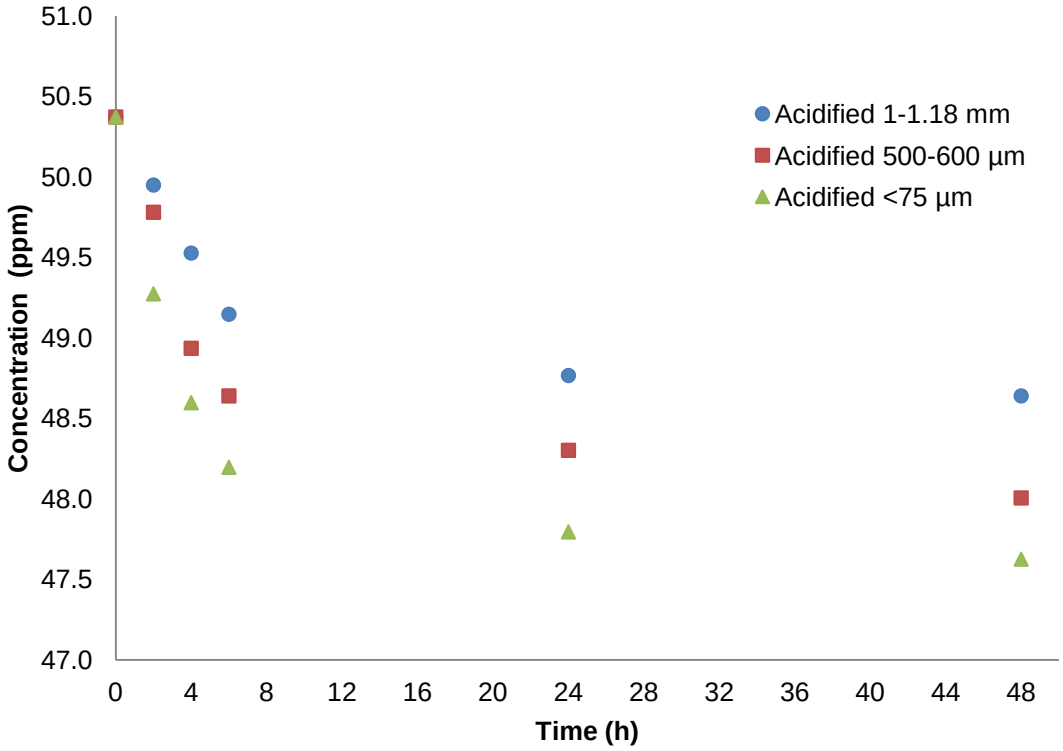

Figure 15. Kinetics of phosphorus sorption on “acidified” laterite for particle sizes: Φ < 75 µm; 500 µm < Φ < 600 µm; and 1 mm < Φ < 1.18 mm.

As observed from figures, in the three experiments carried out the time needed to reach equilibrium was approximately 8 hours, although this is not particularly clear in the last case, when the acidified laterite was used, due to the length of the time intervals selected for taking the samples.

It can also be observed that the reduction in the phosphorus concentration once the equilibrium is reached is relatively low, since the lowest equilibrium concentration is 47.62 ppm (acidified laterite, particle size Φ < 75 µm), which gives a percentage of removal of 5.45% of the initial concentration.

Furthermore, it is clear to see that as the particle size of laterite decreases, the adsorption is done more efficiently. This may be attributed to the fact that diffusion inside the particle is quicker for smaller particle sizes.

All of these conclusions can also be drawn from Table 5, which shows the amount of equilibrium adsorption q_e, calculated through equation (2), for each one of the experiments carried out:

Table 5. Equilibrium adsorption of phosphorus for the three layers and the three particle sizes.

q_e (mg/g)	**Laterite**		
	Lower	**Upper**	**Acidified**
1 mm < Φ < 1.18 mm	1.18	1.52	1.73
500 µm < Φ < 600 µm	1.44	1.90	2.37
Φ < 75 µm	1.69	2.16	2.75

The table above emphasizes again the fact that the best choice for future experiments would be the acidified laterite with the lowest particle size possible, since if we consider all the results from the equilibrium adsorption, the best of them all is 2.75 mg/g, obtained from the acidified laterite and the particle diameter lower than 75 µm (the lowest one in the granulometric distribution of the laterite).

4.3.2. First and Second Order Approximations

In order to predict the kinetic model of the adsorption process, three simultaneous experiments were carried out under the following conditions:

- Temperature: T = 25 ºC (Room temperature).
- Initial concentration of phosphorus [P]: C_0 = 25 ppm.
- Volume of the flasks: V = 1 L.
- Mass of adsorbent (laterite): m = 1 g (Dose = 1 g/L).
- Particle size of the adsorbent: Φ < 75 µm.
- Mass of pH buffer ($NaHCO_3$): 100 mg (Dose = 100 mg/L).
- Initial pH: 7.0 (Constant due to the pH buffer).
- Stirrer speed: 500 rpm (RCT basic IKAMAG® safety control).
- Volume of the samples: 10 mL.
- The samples were taken at the intervals of 0, 1, 2, 3, 4, 5, 6, 7, 8, 24, 28 and 48 hours after the start of the adsorption reaction, and subsequently diluted and analyzed in the spectrophotometer after following the procedure of the colorimetric method.
- For each one of the intervals, the concentration of phosphorus was calculated with equation (15) and later re-calculated considering the dilution factor in order to obtain the real concentration.

Similarly to the preliminary study, this procedure was followed for three different experiments: the first one using the layer of laterite called “lower”, the second one with the layer called “upper”, and the third one with the layer called “acidified”. This was done in order to obtain another comparison between the different kinds of laterite, although this time only the lowest particle size was used.

The results are illustrated in Figure 16:

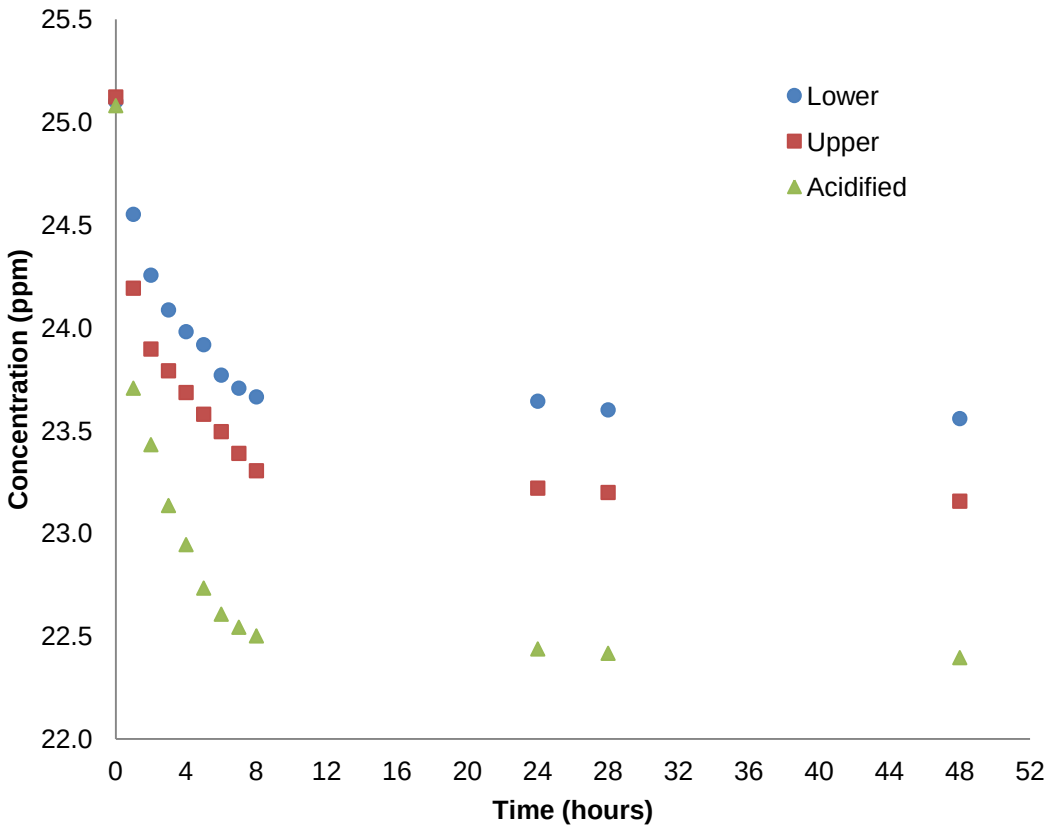

Figure 16. Kinetics of phosphorus sorption on laterite (particle size Φ < 75 µm), for C_0 = 25 ppm, adsorbent dose = 1 g/L and pH = 7.

From the above figure it is clear to see that the acidified laterite is the best choice for future experiments, since it is the kind of laterite that gives the highest percentage of removal of phosphorus. This is probably due to the fact that the acidified laterite has a more porous structure, as suggested in section 4.1. Therefore, from that moment onwards only acidified laterite was used for the rest of experiments in this project.

Phosphate adsorption on laterite consisted of a fast and a slow reaction process. The fast process was completed in approximately 8 hours, in which phosphorus sorption increased rapidly with increasing retention time, whereas the slow process could extend over 48 h. The slow phosphorus sorption process was likely related to the diffusion of adsorbed P into inner surface of the laterite and to the possibility of surface precipitation reactions to form different kinds of iron and aluminium phosphates.

Adsorption kinetic data were subsequently treated in order to obtain a suitable kinetic model, although only the data from acidified laterite were considered, as they gave the highest efficiency in phosphate removal. Figures 17 and 18 show the pseudo-first and pseudo-second order approximations obtained from fitting the experimental data from the acidified laterite to both equations (4) and (6):

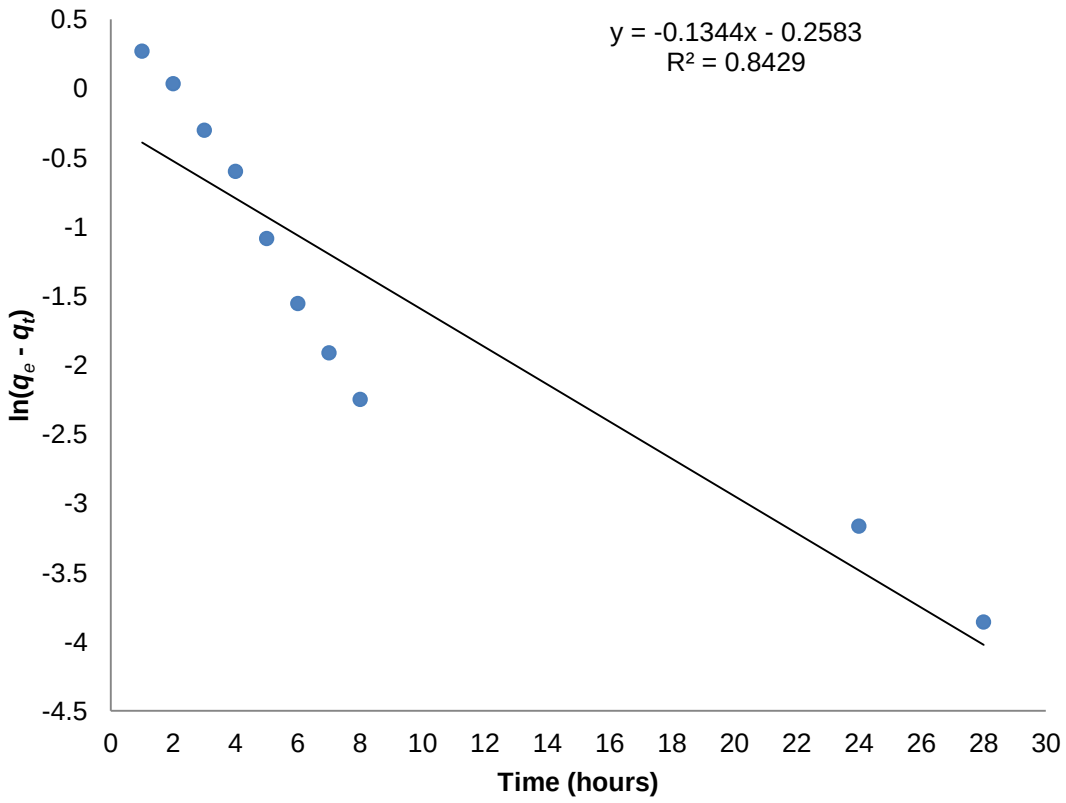

Figure 17. Linear first-order kinetic sorption data for P on acidified laterite (particle size Φ < 75 µm), for C_0 = 25 ppm, adsorbent dose = 1 g/L and pH = 7.

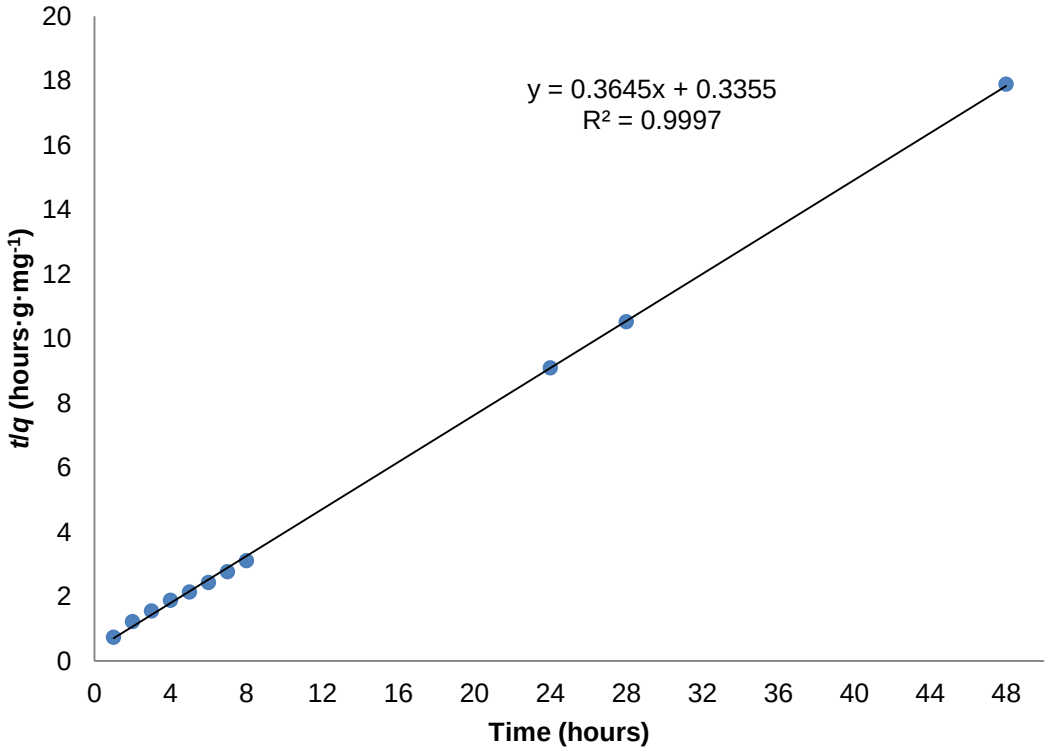

Figure 18. Linear second-order kinetic sorption data for P on acidified laterite (particle size Φ < 75 µm), for C_0 = 25 ppm, adsorbent dose = 1 g/L and pH = 7.

The kinetic parameters from both models are shown in Table 6 below:

Table 6. Comparison of the first- and second-order reaction constants for acidified laterite.

First-order kinetic model			Second-order kinetic model		
k_1 (h^{-1})	q_e	R^2	k_2 (g mg^{-1} h^{-1})	q_e	R^2
0.134	0.772	0.843	0.396	2.743	0.999

The results indicate that the first-order kinetic model is not applicable, since the correlation coefficient (R^2) obtained with this approximation is relatively low. This is due to the fact that near equilibrium the experimental data deviate notably from the previous data obtained during the first stage of the experiment. The correlation coefficient obtained with the second-order approximation is, however, much higher (~1), which shows the suitability of this model.

A good way to compare the model and the experimental data is calculating the relative error between both values of adsorption capacities at equilibrium (q_e), which is shown in Table 7 below:

Table 7. Comparison between experimental and model adsorption capacities.

q_e (mg/g) from experimental data (eq. 2)	q_e (mg/g) from second-order model	Relative error (%)
2.684	2.743	2.198 %

The low value of the relative error (2.198%) between both adsorption capacities again confirms the applicability of the pseudo-second-order kinetic model.

Therefore, the kinetic model that can be applied to the adsorption process of phosphate onto acidified laterite is based in the following equation:

$$\frac{dq}{dt} = 0.396\left(2.743 - q_t\right)^2 \tag{16}$$

Or, alternatively:

$$\frac{t}{q_t} = 0.336 + 0.365\,t \tag{17}$$

Finally, a graph with the experimental and mathematical model data was made –see Figure 19– in order to see the similarity between both models:

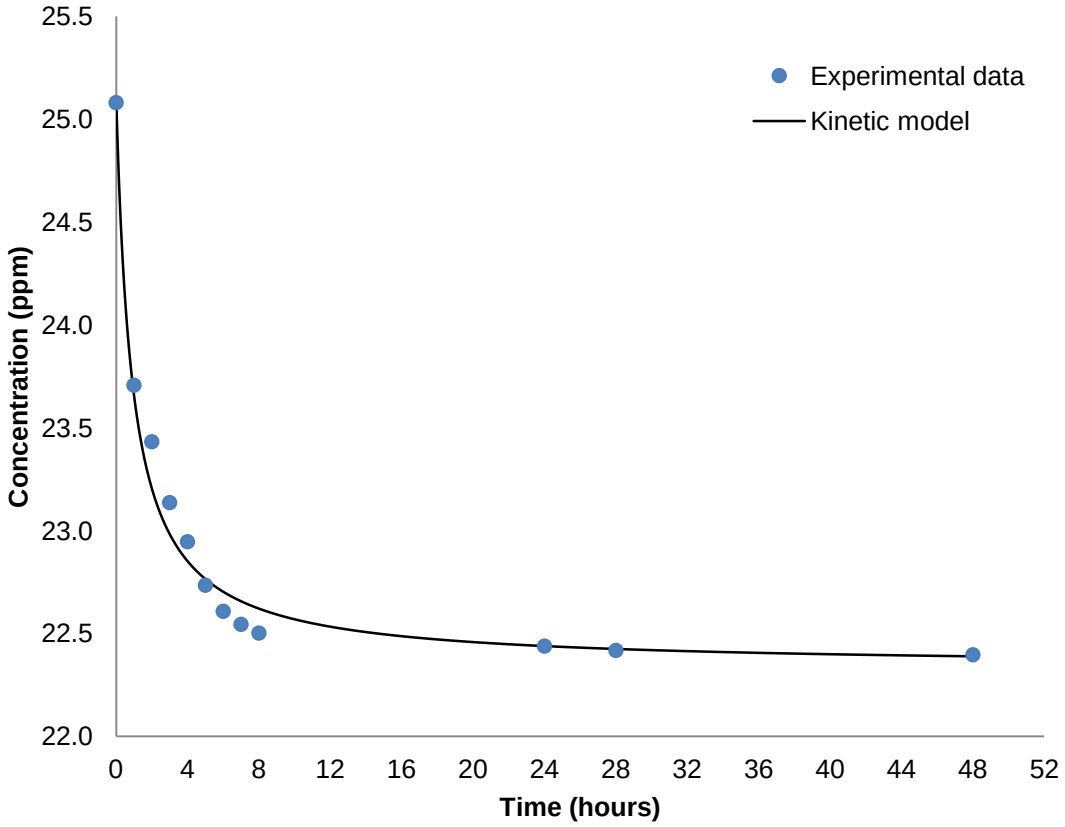

Figure 19. Comparison between experimental and second-order model data for P on acidified laterite (particle size Φ < 75 µm), for C_0 = 25 ppm, adsorbent dose = 1 g/L and pH = 7.

From the above figure it is clear to see that the pseudo-second-order model fits relatively well with the experimental data, with only slight differences in the first stage of the adsorption (fast stage). We can therefore conclude that this model is perfectly applicable to predict the kinetics of the phosphorus adsorption onto acidified laterite.

4.4. Adsorption Isotherms

4.4.1. Effect of Initial Concentration

Phosphate adsorption isotherm studies were carried out under the following conditions:

- Temperature: T = 25 ºC (Room temperature).
- Volume of the flasks: V = 50 mL.
- Mass of adsorbent ("acidified" laterite): m = 50 mg (Dose = 1 g/L).
- Particle size of the adsorbent: Φ < 75 µm.
- Mass of pH buffer ($NaHCO_3$): 100 mg (Dose = 100 mg/L).
- Initial pH: 7.0 (Constant due to the pH buffer).
- Shaker: Gerhardt Bonn LS/RO500 type 655.

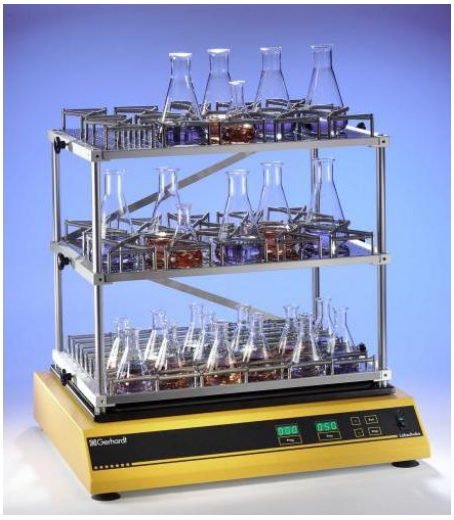

Figure 20. Gerhardt Bonn LS/RO500 type 655 shaker.

- Time of reaction: 72 h.
- Volume of the samples: 10 mL.
- Once the samples were filtered, the concentration of phosphorus in the equilibrium (C_e) of each one of them was calculated with equation (15) and later re-calculated considering the dilution factor in order to obtain the real concentration.
- Furthermore, for each one of the samples, the quantity of adsorbed phosphorus (q_e) was subsequently calculated with equation (2).

This procedure was followed for eight different initial concentrations (C_0) of phosphorus: 5, 10, 15, 20, 25, 30, 40 and 50 ppm.

The results of the phosphate adsorption isotherm experiments are shown in Figures 21a and 21b:

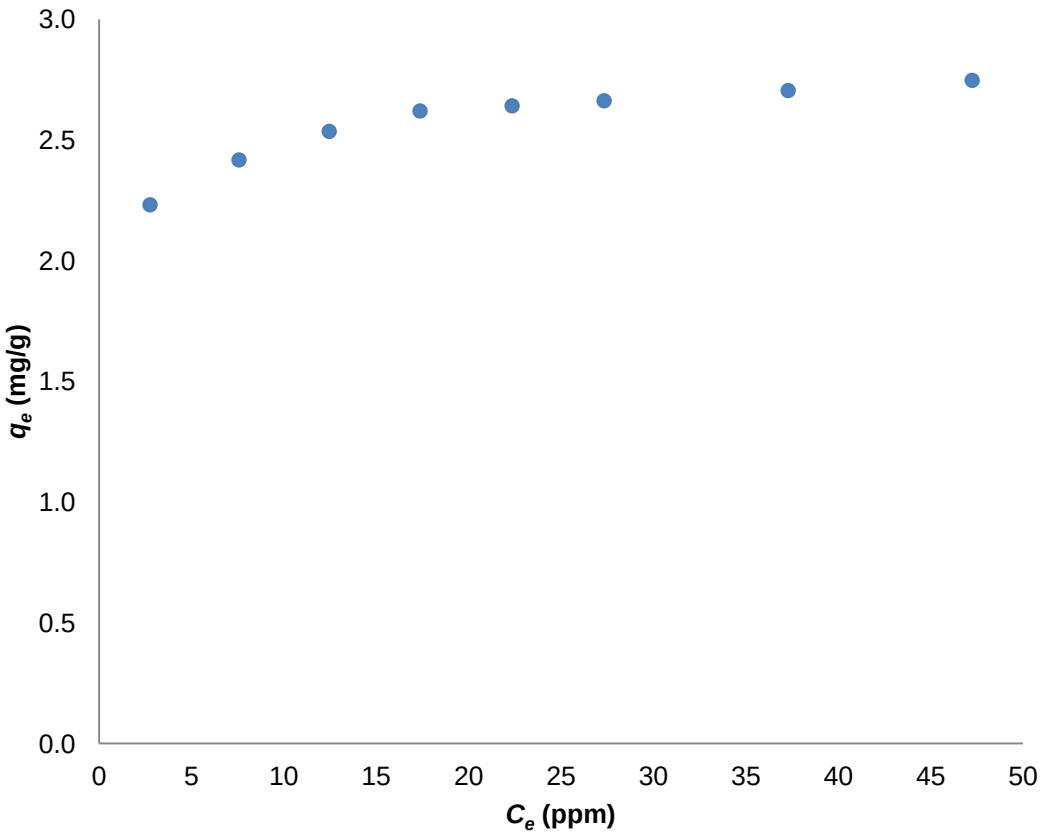

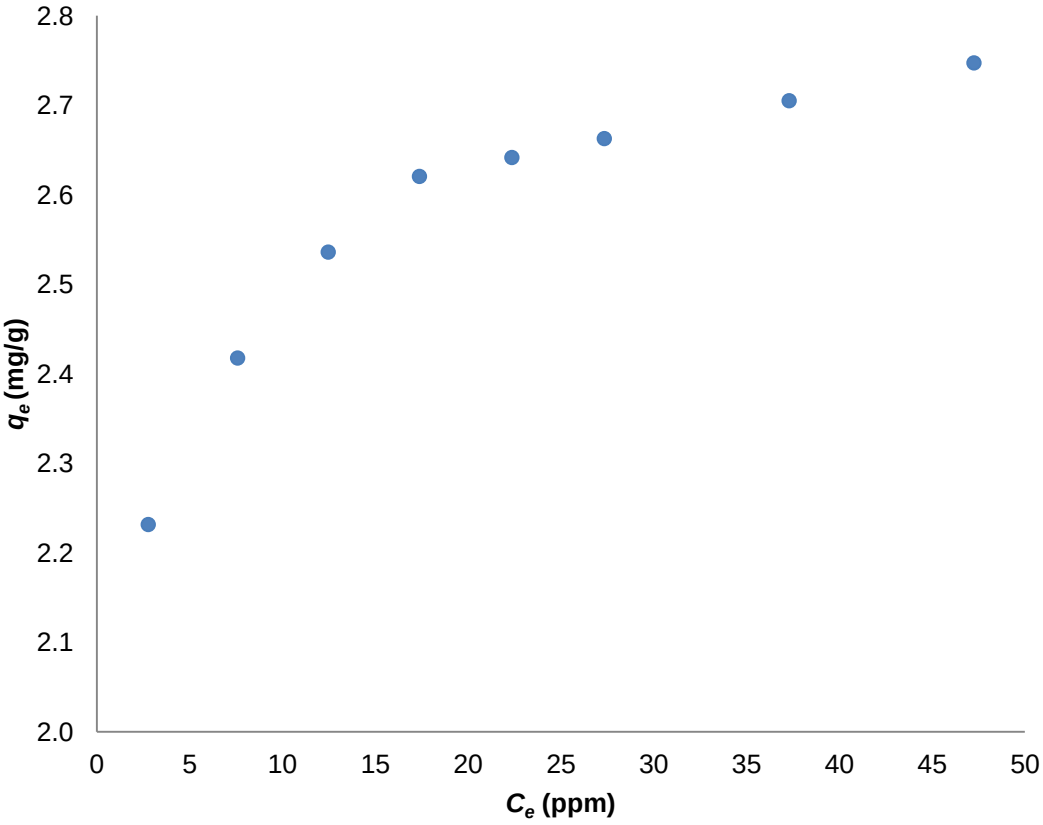

Figures 21a and 21b. Phosphorus adsorption isotherm for acidified laterite.
Particle size: Φ < 75 µm; temperature = 25 ºC; adsorbent dose = 1 g/L; pH = 7.

The experimental isotherm data can be characterized by the typical L-curve isotherm, in which the initial slope does not significantly change with the solute concentration. Even so, this cannot be confirmed because of the lack of data within the range from 0 to 5 ppm, due to limitations in the range of concentrations with which the phosphorus calibration curve was done (see Figure 21b).

Phosphorus adsorption capacity significantly increased with the phosphorus concentration increasing from 5 to 20 ppm. This capacity was approximately 2.6 mg/g for a phosphorus equilibrium concentration of 20 ppm. Nevertheless, with a further increase of the phosphorus equilibrium concentration, the increase of adsorption was less significant, as it only increased until 2.75 mg/g for an equilibrium concentration of 47.25 ppm.

Even so, the general results from the adsorption capacity can be considered low, and better results in terms of percentage of removal are expected with an increasing of the dose of laterite, as the highest percentage of removal was approximately 44%, obtained with the lowest value of the phosphorus equilibrium concentration (see Figure 22 below).

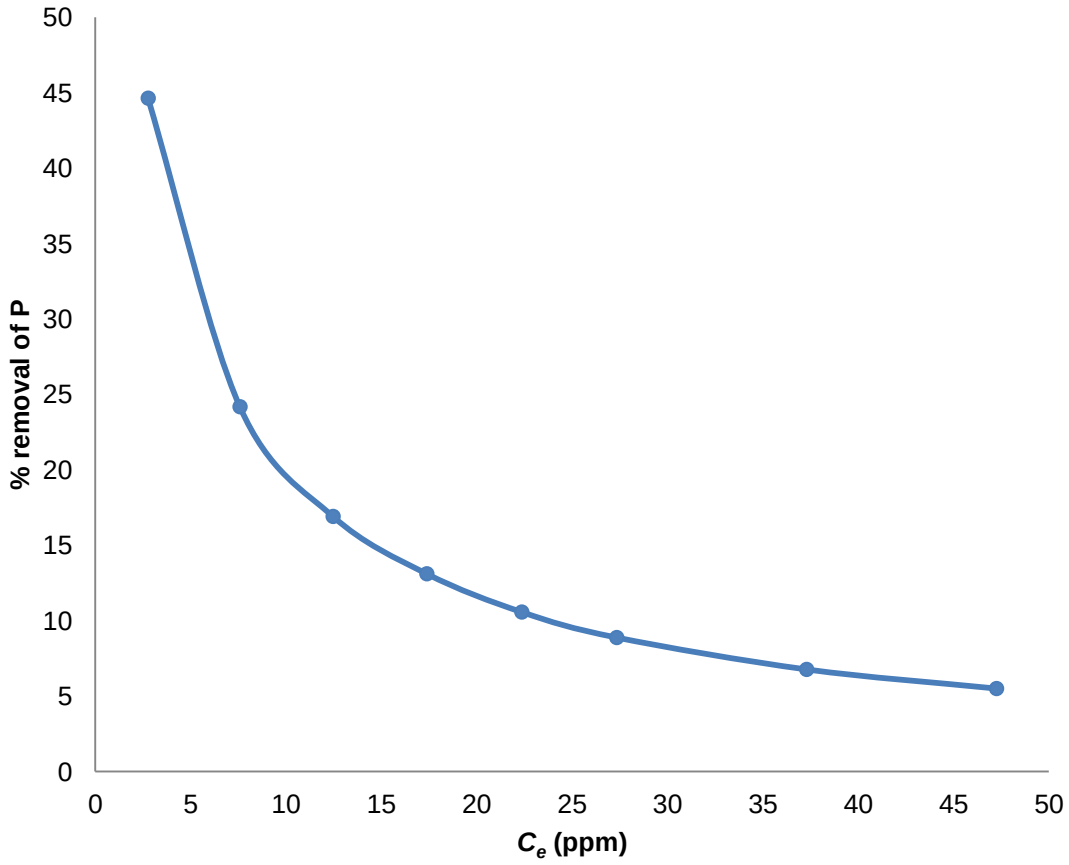

Figure 22. Percentage of removal of P for acidified laterite (particle size Φ < 75 µm). Temperature = 25 ºC; adsorbent dose = 1 g/L; pH = 7.

4.4.2. Freundlich and Langmuir Isotherms

The adsorption data were analyzed using the Freundlich and Langmuir models as outlined in section 3.3. In order to compare both isotherms, two graphs were plotted over the concentration range, whose results are illustrated in Figures 23 and 24 below:

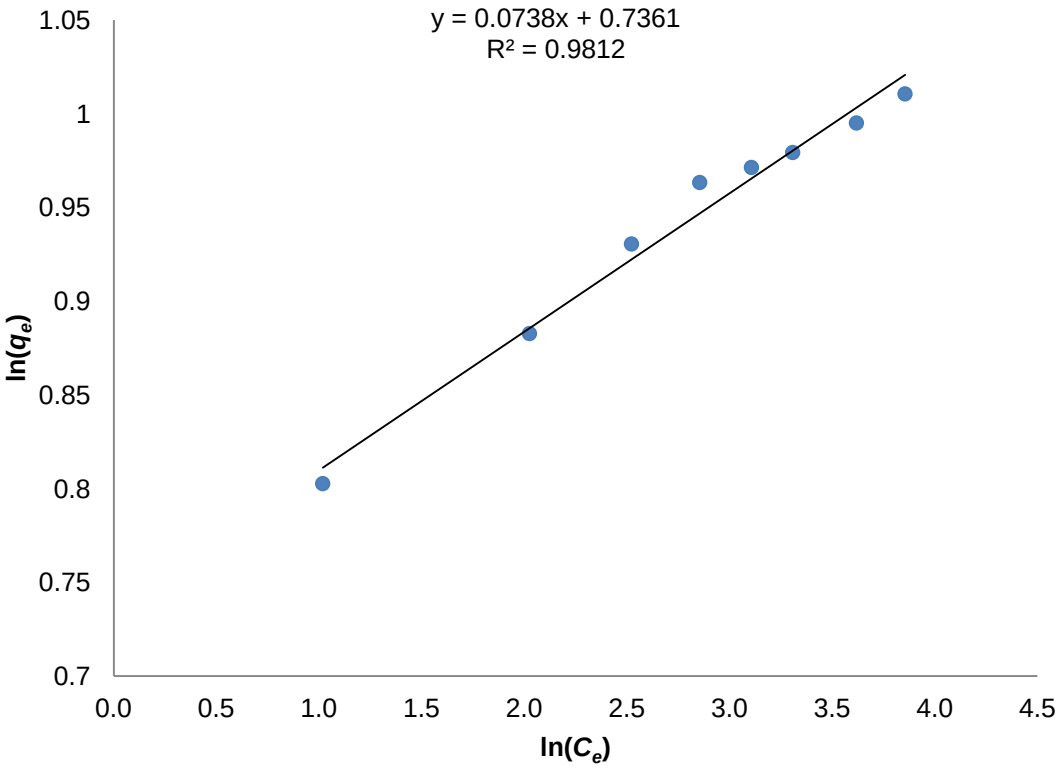

Figure 23. Freundlich linear isotherm data for P adsorption on acidified laterite. Particle size: Φ < 75 µm; temperature = 25 ºC; adsorbent dose = 1 g/L; pH = 7.

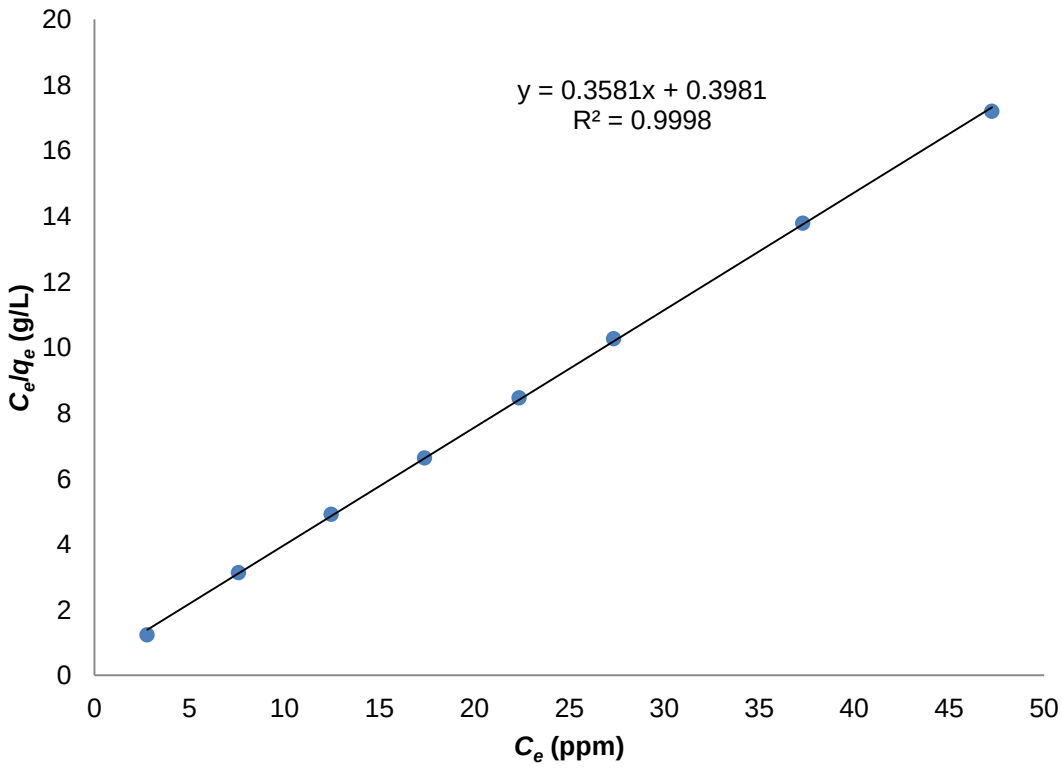

Figure 24. Langmuir linear isotherm data for P adsorption on acidified laterite. Particle size: Φ < 75 µm; temperature = 25 ºC; adsorbent dose = 1 g/L; pH = 7.

The estimated values of P adsorption parameters obtained from these models are shown in Table 8:

Table 8. Freundlich and Langmuir adsorption constants for P adsorption on acidified laterite.

Freundlich model			**Langmuir model**		
K_F	n	R^2	K_L (L/mg)	Q_0 (mg/g)	R^2
2.088	13.550	0.981	0.900	2.793	0.999

The experimental data fitted well the Freundlich and Langmuir equations, with correlation coefficients ranging from 0.981 to 0.999 (~1).

Similar results were obtained regarding P sorption capacity (K_F and Q_0 values), although the value of Q_0 is more reliable due to the comparison with the approximated value that can be obtained directly from the experimental data –see Figure 21– and also because the value of the correlation coefficient is slightly higher for the Langmuir model.

On the other hand, the parameters n and K_L are not directly comparable. The constant n refers to the interaction between exchange sites in the adsorbent and P ions. A high value for $n > 1$ –as the one obtained– indicates favourable adsorption. The K_L in the Langmuir model measures the affinity of the adsorbent for the solute, this means that a higher value of K_L refers to a higher adsorption level at low solution concentration. Even so, the Langmuir isotherm shape can be classified by a term R_L, a dimensional constant separation factor, using equation (18);

$$R_L = \frac{1}{1 + K_L C_0} \tag{18}$$

the value of which indicates the nature of the adsorption process, as shown in Table 9:

Table 9. R_L value definitions.

R_L value	**Nature of adsorption process**
$R_L > 1$	Unfavourable
$R_L = 1$	Linear
$0 < R_L < 1$	Favourable
$R_L = 0$	Irreversible

The values obtained are shown in Table 10 below:

Table 10. R_L values for P adsorption on acidified laterite.

C_0 (ppm)	**R_L value**	**Nature of adsorption process**
5	0.182	Favourable
10	0.100	Favourable
15	0.069	Favourable
20	0.053	Favourable
25	0.043	Favourable
30	0.036	Favourable
40	0.027	Favourable
50	0.022	Favourable

The results again confirm that the adsorption was a highly favourable process over the concentration range. Furthermore, it may be noted that all the values are close to zero, suggesting proximity to irreversibility.

In order to establish a mathematical model for the isotherm, the Langmuir equation was applied, since the highest value of the correlation coefficient was obtained with such model. Therefore, the isotherm that can be applied to the adsorption process of phosphate onto acidified laterite is based in the following equation:

$$q_e = \frac{2.512\, C_e}{1 + 0.9\, C_e} \tag{19}$$

Finally, a graph with the experimental and Langmuir model data was made in order to confirm the similarity between both models, as shown in Figure 25 below:

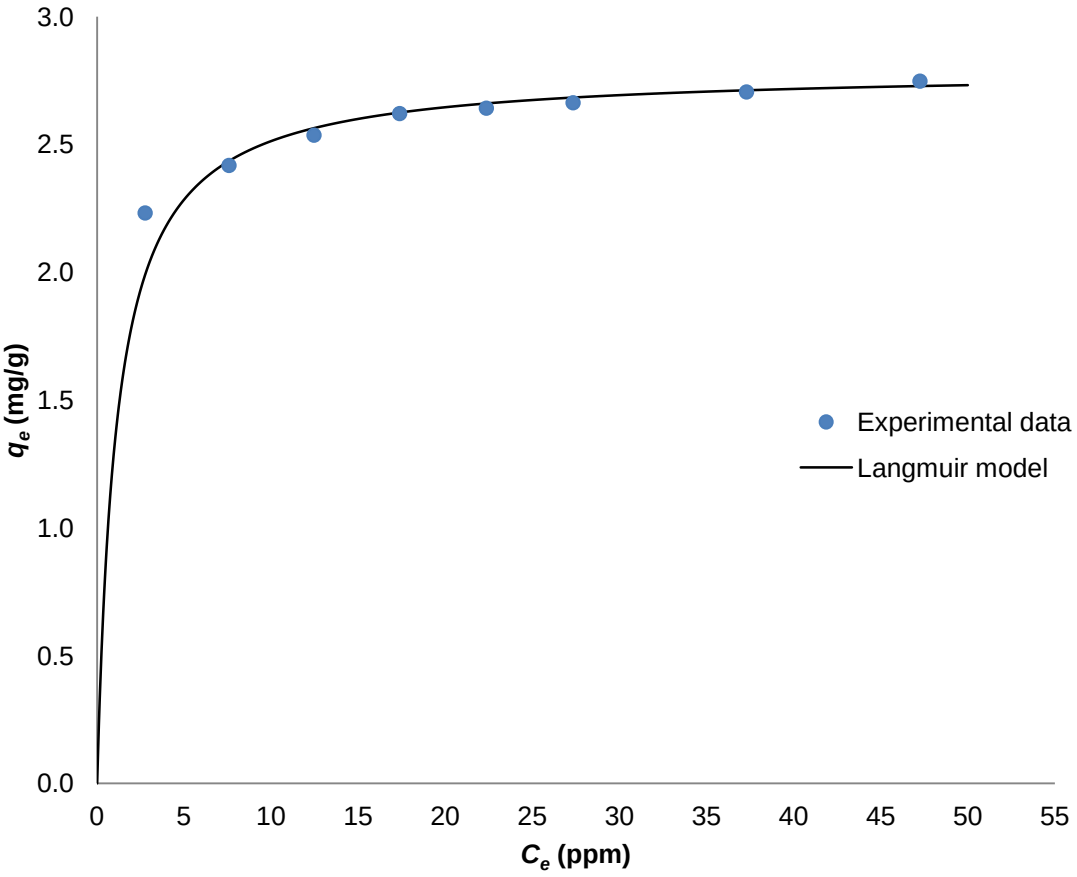

Figure 25. Comparison between experimental and Langmuir model data for P adsorption on acidified laterite (particle size: Φ < 75 µm). Temp. = 25 ºC; adsorbent dose = 1 g/L; pH = 7.

From the above figure, it can be concluded that the Langmuir model fits relatively well with the experimental data in terms of shape, with only slight deviations for the lowest concentration data within the working range.

4.4.3. Effect of Temperature

Temperature normally has important effects on an adsorption process. In order to see the variation in parameters such as the adsorption capacity or the percentage of removal, three different isotherms were carried out at the temperatures of 303, 313 and 323 K. The procedure followed was exactly the same as that one described in section 4.4.2, with the only difference that the flasks were placed into a temperature controlled water bath –see Figure 26 below– with agitation, and again left for 72 hours.

Figure 26. Lifton NE5-28 Analogue Shaking Water Bath.

Once the results from the colorimetric method were obtained, the experimental data were plotted along with the isotherm at room temperature (298 K) obtained in section 4.4.2. A comparison between the four isotherms can be seen in Figure 27:

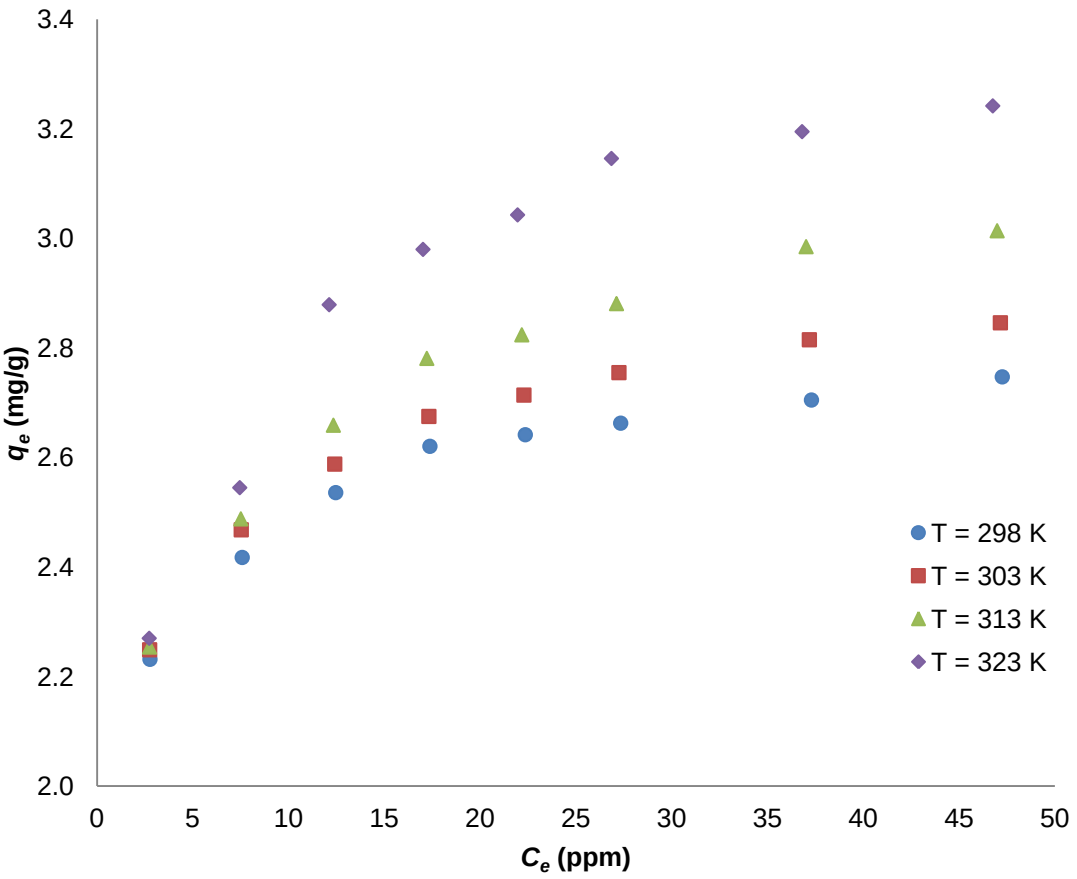

Figure 27. Isotherms obtained at 298, 303, 313 and 323 K for P adsorption on acidified laterite. Particle size: Φ < 75 µm; adsorbent dose = 1 g/L; pH = 7.

As seen in the figure above, an increase in the temperature has a positive effect in the maximum adsorption capacity of the laterite, ranging between approximately 2.75 mg/g for the lowest value of temperature (298 K) and 3.24 mg/g for the highest one (323 K). This is equivalent to a 17.82% growth in the maximum adsorption capacity.

These values suggest that phosphorus adsorption on laterite must be an endothermic process, as it was found in literature of phosphorus adsorption onto inorganic adsorbents, for example, electrocoagulated metal hydroxides sludge, iron oxide coated sand and kaolinite.

It is also interesting to see the changes in terms of percentage of removal of phosphorus, as outlined in Table 11:

Table 11. Effect of the temperature in the percentage of removal of P on acidified laterite.

C_0 (mg/L)	% removal of P			
	***T* = 298 K**	***T* = 303 K**	***T* = 313 K**	***T* = 323 K**
5	44.63	44.98	45.08	45.40
10	24.18	24.68	24.88	25.45
15	16.91	17.25	17.73	19.19
20	13.10	13.38	13.91	14.90
25	10.57	10.86	11.30	12.17
30	8.88	9.18	9.60	10.49
40	6.76	7.04	7.46	7.99
50	5.49	5.69	6.03	6.48

Although it is clear that the % of removal of P increases with increasing process temperature, the variation is not as high as that one observed for the maximum adsorption capacity, since it only changes –at the very best– from 44.63% to 45.40%, considering the data obtained from the lowest initial phosphorus concentration.

Finally, the experimental data were fitted to the Langmuir isotherm as done in section 4.4.2, in order to obtain mathematical models that can be applied to the adsorption of phosphorus on laterite at different temperatures. The results are outlined in Table 12 and Figure 28:

Table 12. Langmuir constants for P adsorption on acidified laterite at different temperatures.

T (K)	Langmuir model			
	K_L (L/mg)	Q_0 (mg/g)	R^2	Equation
298	0.900	2.793	0.999	$q_e = \frac{2.512\,C_e}{1+0.9\,C_e}$
303	0.749	2.910	0.999	$q_e = \frac{2.181\,C_e}{1+0.749\,C_e}$
313	0.552	3.109	0.999	$q_e = \frac{1.717\,C_e}{1+0.552\,C_e}$
323	0.500	3.367	0.999	$q_e = \frac{1.682\,C_e}{1+0.5\,C_e}$

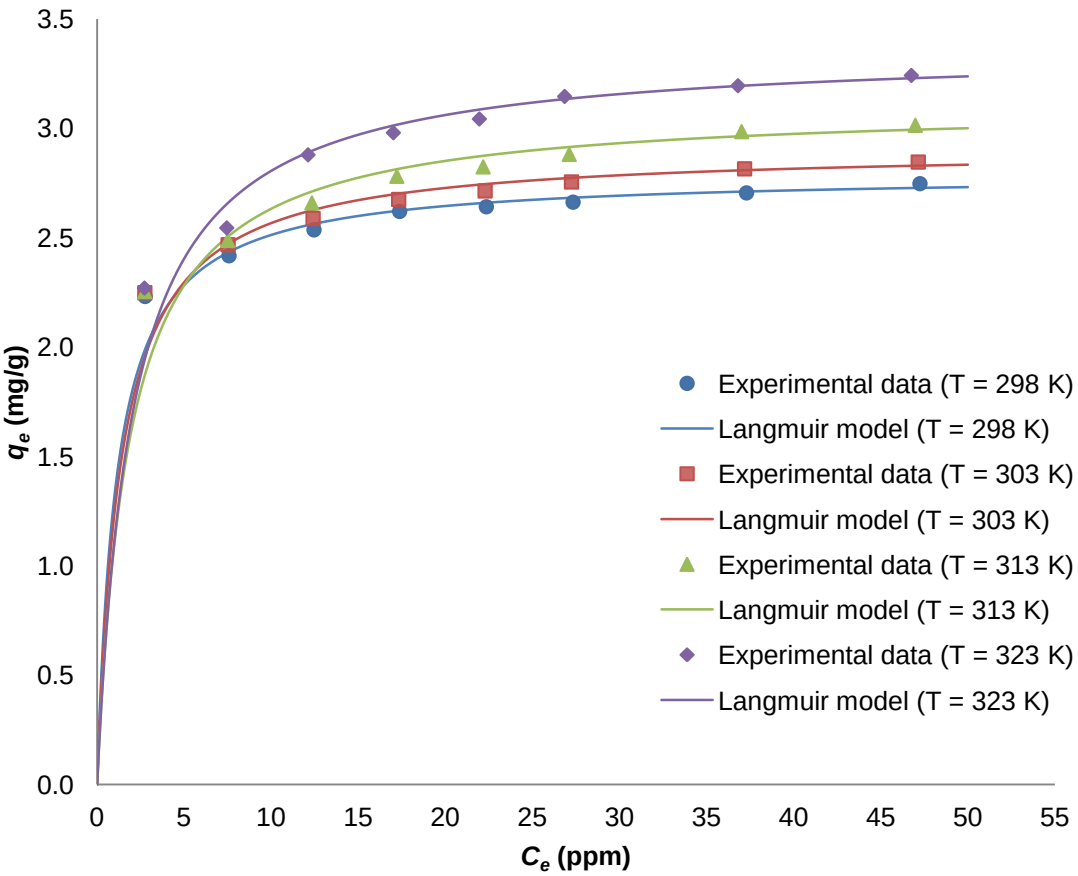

Figure 28. Isotherms obtained at 298, 303, 313 and 323 K for P adsorption on acidified laterite. Particle size: Φ < 75 µm; adsorbent dose = 1 g/L; pH = 7.

The increase of the maximum adsorption capacity of the laterite with the temperature is again confirmed with the parameters Q_0 obtained with the Langmuir model, ranging from 2.793 to 3.367 mg/g. The fact that the adsorption of phosphorus on laterite can be considered an endothermic process is also tested in the next section.

4.4.4. Thermodynamic Parameters

The values of the thermodynamic parameters for the adsorption process of phosphorus on acidified laterite were determined applying the method described in section 3.4 for the experimental data obtained from the four experiments –at four different temperatures– carried out in section 4, although only the highest phosphorus concentration (50 ppm) was considered for this study.

The results obtained from the van't Hoff equation are shown in Figure 29 below:

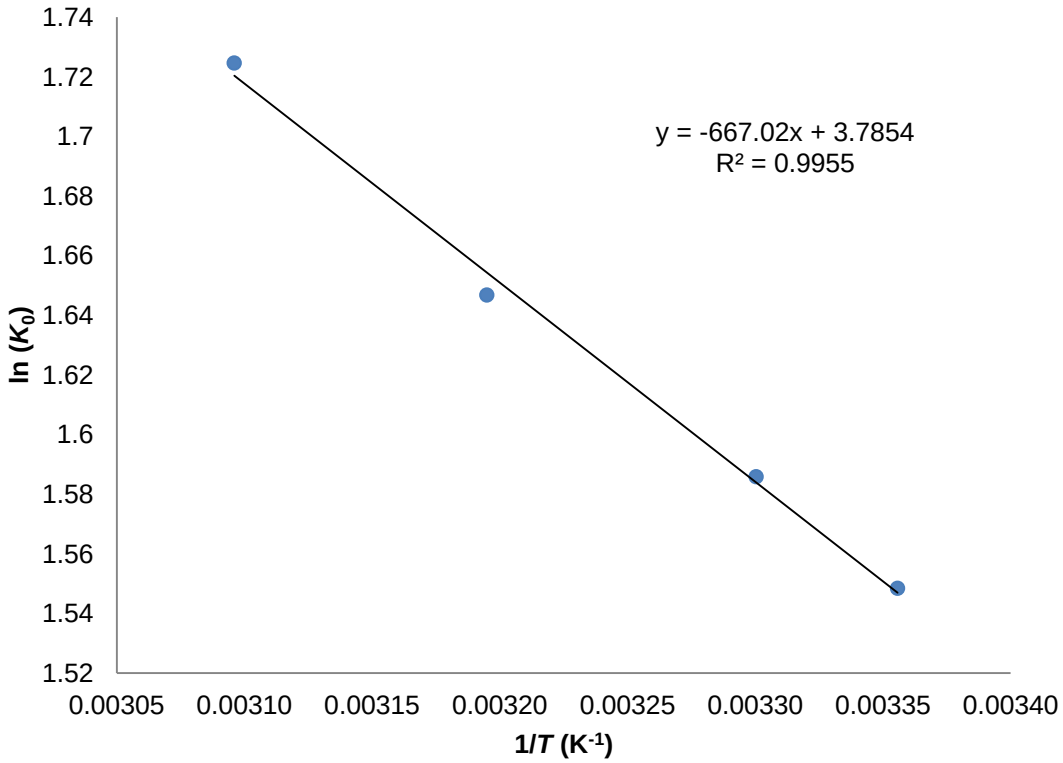

Figure 29. Plot of ln(K_0) vs (1/T) for estimation of thermodynamic parameters for P adsorption on acidified laterite. Particle size: Φ < 75 µm; adsorbent dose = 1 g/L; pH = 7; C_0 = 50 ppm.

The thermodynamic parameters were obtained from the slope and intercept of the graph above and they are outlined in Table 13:

Table 13. Thermodynamic parameters for P adsorption on acidified laterite.
Particle size: Φ < 75 µm; adsorbent dose = 1 g/L; pH = 7; C_0 = 50 ppm.

***T* (K)**	**Thermodynamic parameters**		
	(ΔH^0) (kJ/mol)	**(ΔS^0) (J mol^{-1} K^{-1})**	**(ΔG^0) (kJ/mol)**
298	5.545	-5.055	-3.836
303			-3.995
313			-4.285
323			-4.631

The positive value of the enthalpy change (ΔH^0) confirms that the adsorption of this work is an endothermic reaction, as suggested in section 4.4.3, while the negative value of the entropy change (ΔS^0) shows the decreasing randomness at the solid/liquid interface during the sorption of phosphorus onto laterite. Finally, the negative value of Gibbs free energy (ΔG^0) indicates the feasibility of the process and the spontaneous nature of adsorption.

4.5. Effect of Adsorbent Dose

Some studies were made in order to see the influence of the adsorbent dosage in the adsorption capacity of the laterite and the percentage of removal of phosphorus. These experiments were made under the following conditions:

- Temperature: T = 25 ºC (Room temperature).
- Initial concentration of phosphorus [P]: C_0 = 25 ppm.
- Volume of the flasks: V = 100 mL.
- Particle size of the adsorbent: Φ < 75 µm.
- Mass of pH buffer ($NaHCO_3$): 100 mg (Dose = 100 mg/L).
- Initial pH: 7.0 (Constant due to the pH buffer).
- Shaker: Gerhardt Bonn LS/RO500 type 655.
- Time of reaction: 72 h.
- Volume of the samples: 10 mL.
- Once the samples were filtered, the concentration of phosphorus in the equilibrium (C_e) of each one of them was calculated with equation (15) and later re-calculated considering the dilution factor in order to obtain the real concentration.
- Furthermore, for each one of the samples, the quantity of adsorbed phosphorus (q_e) was subsequently calculated with equation (2).

This procedure was followed for eight different adsorbent doses of “acidified” laterite, as shown in Table 14 below:

Table 14. Adsorbent doses and mass of laterite used for the dose study.

Adsorbent dose (g/L)	**Mass of “acidified” laterite, *m* (mg)**
1	100
2	200
3	300
4	400
5	500
6	600
7	700
8	800

The results from the experiments are outlined in Figures 30 and 31 below:

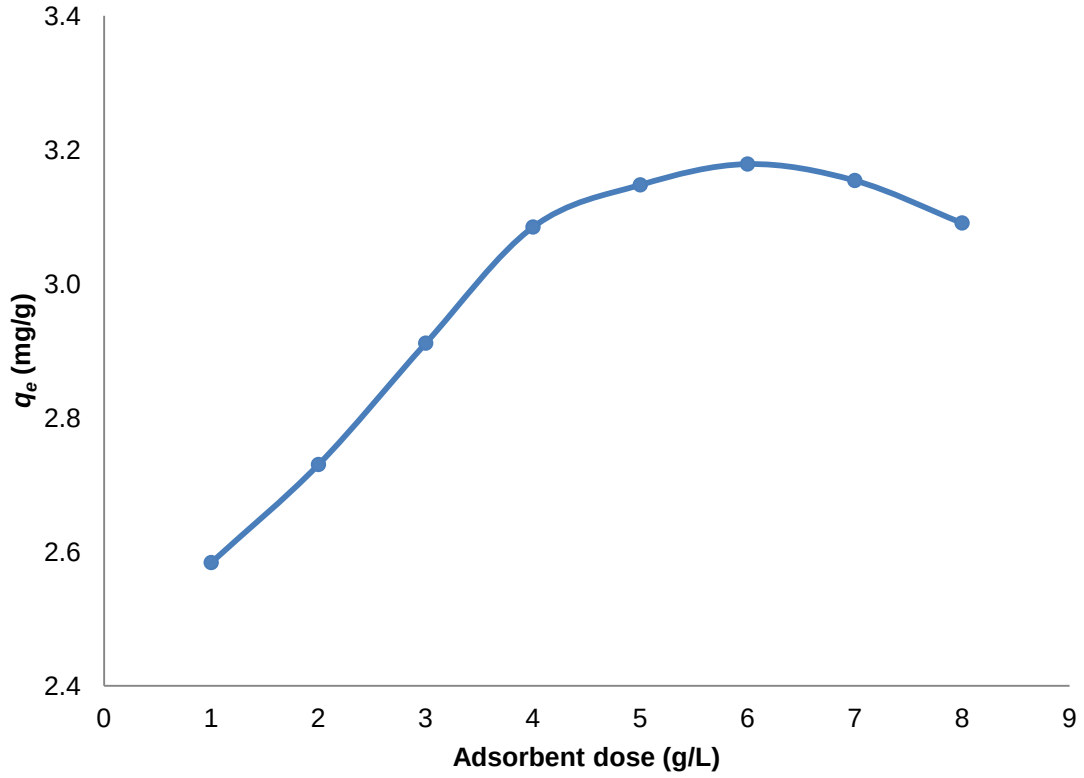

Figure 30. Effect of adsorbent dose on adsorption capacity of acidified laterite for P adsorption. Particle size: Φ < 75 µm; C_0 = 25 ppm; pH = 7.

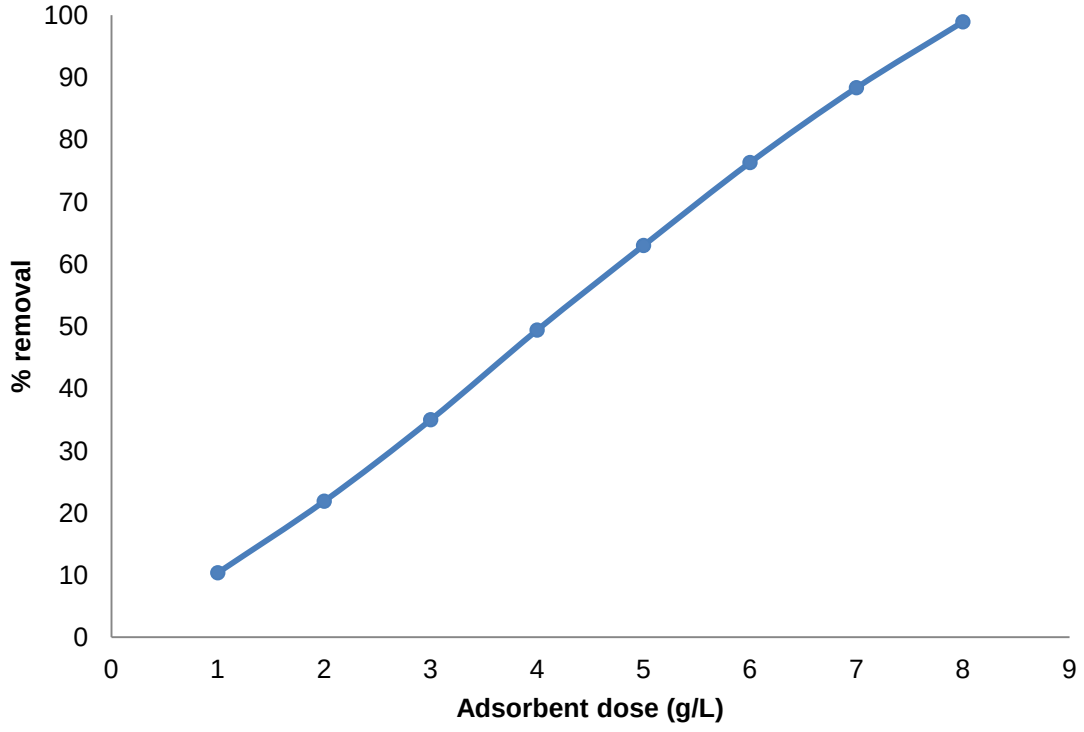

Figure 31. Effect of adsorbent dose on percentage of removal of P on acidified laterite. Particle size: Φ < 75 µm; C_0 = 25 ppm; pH = 7.

From Figure 30, it could be seen that adsorption capacity was found to increase proportionally with an increase in the amount of laterite, with a maximum adsorption capacity of approximately 3.18 mg/g for an adsorbent dosage of 6 g/L. Following decrease in adsorption capacity is attributable to the splitting effect of the concentration gradient between adsorbate and adsorbent, with increased laterite concentration causing a decrease in amount of phosphorus adsorbed onto unit weight of laterite.

Regarding Figure 31, it is clear to see that the removal is more efficient for higher adsorbent dose due to availability of more adsorption sites. It may be noted here that for adsorbent dose of 8 g/L and feed concentration of 25 ppm of phosphorus, the final concentration falls to a level of approximately 1 ppm -due to a percentage of removal of 98.9%-, which is very near to the EC UWWT Directive 100 µg P L^{-1} criteria highlighted in section 2.2 regarding eutrophication in Northern Irish rivers. This may also explain the decrease in adsorption capacity for high adsorbent dosages, since for these cases there is not any phosphate left that can be adsorbed –the percentage of removal is 100%–, resulting in a lower adsorption capacity.

4.6. Effect of Initial pH

The pH of the aqueous solution is an important variable that influences the adsorption of anions and cations at the solid-liquid interfaces. In order to observe the effect of pH on adsorption of phosphorus, a series of experiments were carried out under the following conditions:

- Temperature: T = 25 ºC (Room temperature).
- Initial concentration of phosphorus [P]: C_0 = 10 ppm.
- Volume of the flasks: V = 50 mL.
- Mass of adsorbent ("acidified" laterite): m = 50 mg (Dose = 1 g/L).
- Particle size of the adsorbent: Φ < 75 µm.
- Mass of pH buffer ($NaHCO_3$): 100 mg (Dose = 100 mg/L).
- Shaker: Gerhardt Bonn LS/RO500 type 655.
- Time of reaction: 72 h.
- Volume of the samples: 10 mL.
- Once the samples were filtered, the concentration of phosphorus in the equilibrium (C_e) of each one of them was calculated with equation (15) and later re-calculated considering the dilution factor in order to obtain the real concentration.
- Furthermore, for each one of the samples, the quantity of adsorbed phosphorus (q_e) was subsequently calculated with equation (2).

This procedure was followed for fifteen different initial pH values (pH_0) of the phosphorus aqueous solution: 3.0, 3.5, 4.0, 4.5, 5.0, 5.5, 6.0, 6.5, 7.0, 7.5, 8.0, 8.5, 9.0, 9.5 and 10. The pH of every suspension was adjusted to desired value using HCl or NaOH solutions as described in section 3.1 and kept constant due to the pH buffer, while the pH value was measured with an Orion 3-Star™ Plus Portable pH Meter.

Figure 32. Orion 3-Star™ Plus Portable pH Meters.

The results of these experiments are outlined in Figure 33, which shows the adsorption capacity of the acidified laterite versus the final pH (pH_f) of the solution:

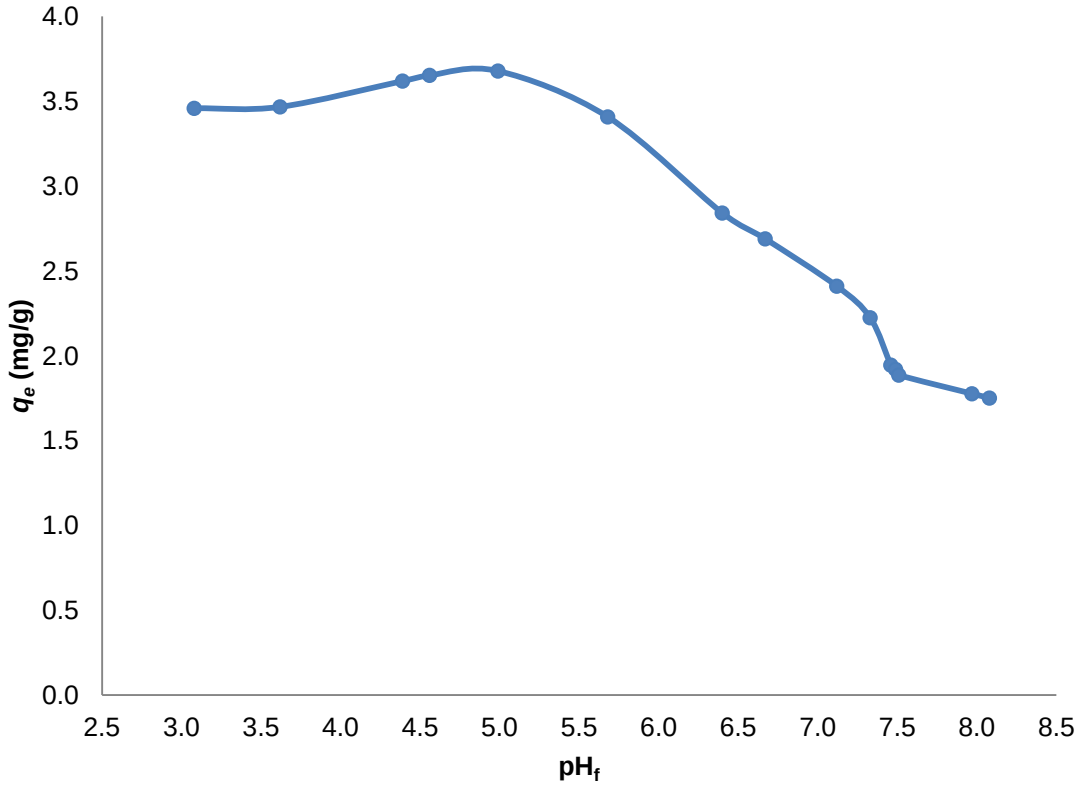

Figure 33. Effect of final pH on phosphorus adsorption onto acidified laterite. Particle size: Φ < 75 µm; C_0 = 10 ppm; pH = 7.

As seen in figure above, the process is clearly pH dependent, which indicates that electrostatic interactions and chemisorption might be involved in the adsorption mechanism of phosphorus on laterite.

The amount of phosphorus adsorbed on laterite was found to be nearly constant at low pH values (below 5.0), with q_e values between 3.46 mg/g and 3.68 mg/g. This can be explained considering that for low pH values the surface of the laterite is surrounded by high quantities of hydronium ions (H_3O^+), and therefore positively charged, which will attract the negative charged phosphate ions. More specifically, in the pH range of 3-5 the predominant specie is the dihydrogen phosphate ion ($H_2PO_4^-$), as can be observed in Figure 34:

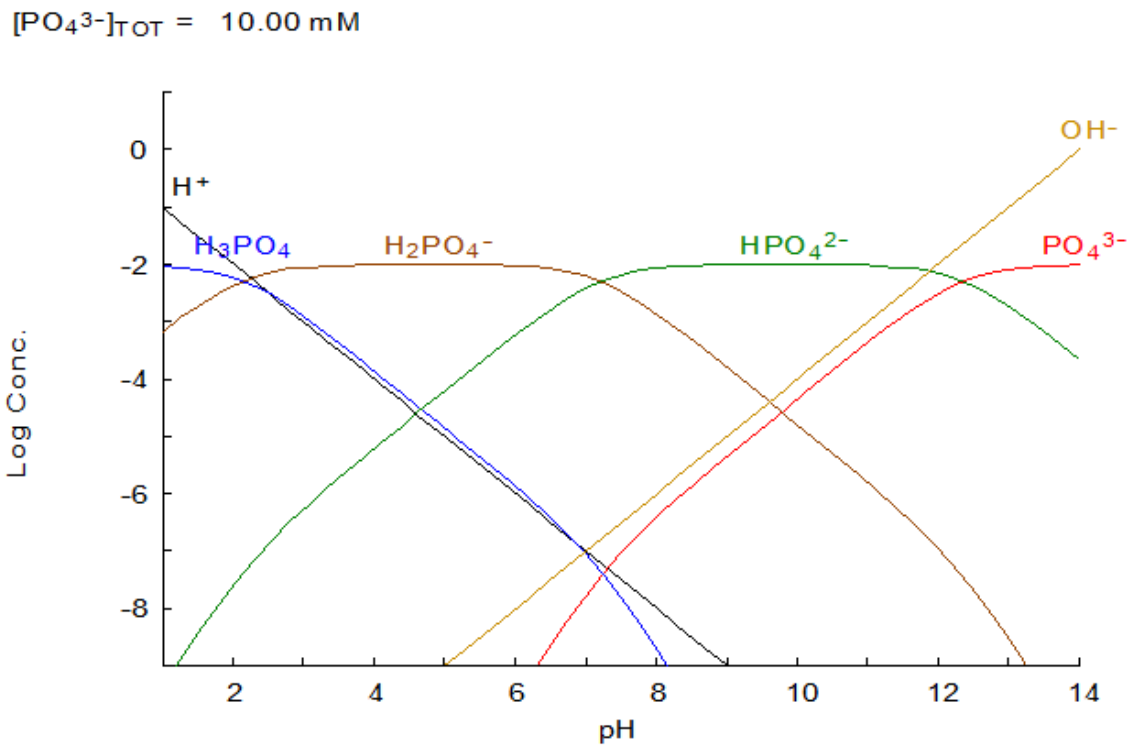

Figure 34. Phosphoric acid speciation for a total phosphate concentration of 10 mM. Source: Medusa Software (Royal Institute of Technology).

On the other hand, for high pH values the adsorption capacity of laterite decreases until 1.94 mg/g (at pH 8.0), which can be attributed to the competition between hydroxyl ions (OH^-) and phosphate ions for adsorption sites.

Another way to justify this change in the adsorption capacity from the pH region between 5.0-5.5 is the point of zero charge (pzc) of the acidified laterite, which was found to be approximately at pH_{pzc} = 5.2, as seen in section 4.1. Therefore, at pH values lower than pH_{pzc}, laterite surface is positively charged, attracting more easily anions such as phosphate, while above this value the surface is negatively charged, repelling anions.

4.7. Column Studies

The last experiments of the project were some column studies, which are different from the rest of the experiments previously done because they are based on dynamic processes instead of batch processes. In these column studies three different flow rates were tested. The rest of the conditions were as follows:

- Temperature: T = 25 ºC (Room temperature).
- Initial concentration of phosphorus [P]: C_0 = 10 ppm.
- Initial volume of influent: 900 mL.
- Mass of pH buffer ($NaHCO_3$): 100 mg (Dose = 100 mg/L).
- Initial pH: 7.0 (constant due to the pH buffer).
- Mass of adsorbent (“acidified” laterite): m = 6 g.
- Particle size of the adsorbent: 500 µm < Φ < 600 µm.
- Bed volume: BV = 9 mL.
- Peristaltic pump: Watson-Marlow 503S.
- Flow rates: Q_1 = 2 mL/min; Q_2 = 4 mL/min; Q_3 = 6 mL/min.

Figure 35. Colum adsorption system.

- Volume of the samples: 9 mL.
- For each one of the samples, the concentration of phosphorus was detected with ICP-AES. The colorimetric method was not applied in this case due to lack of time.

The breakthrough curves of phosphorus on acidified laterite for the different flow rates are presented in Figure 36 below:

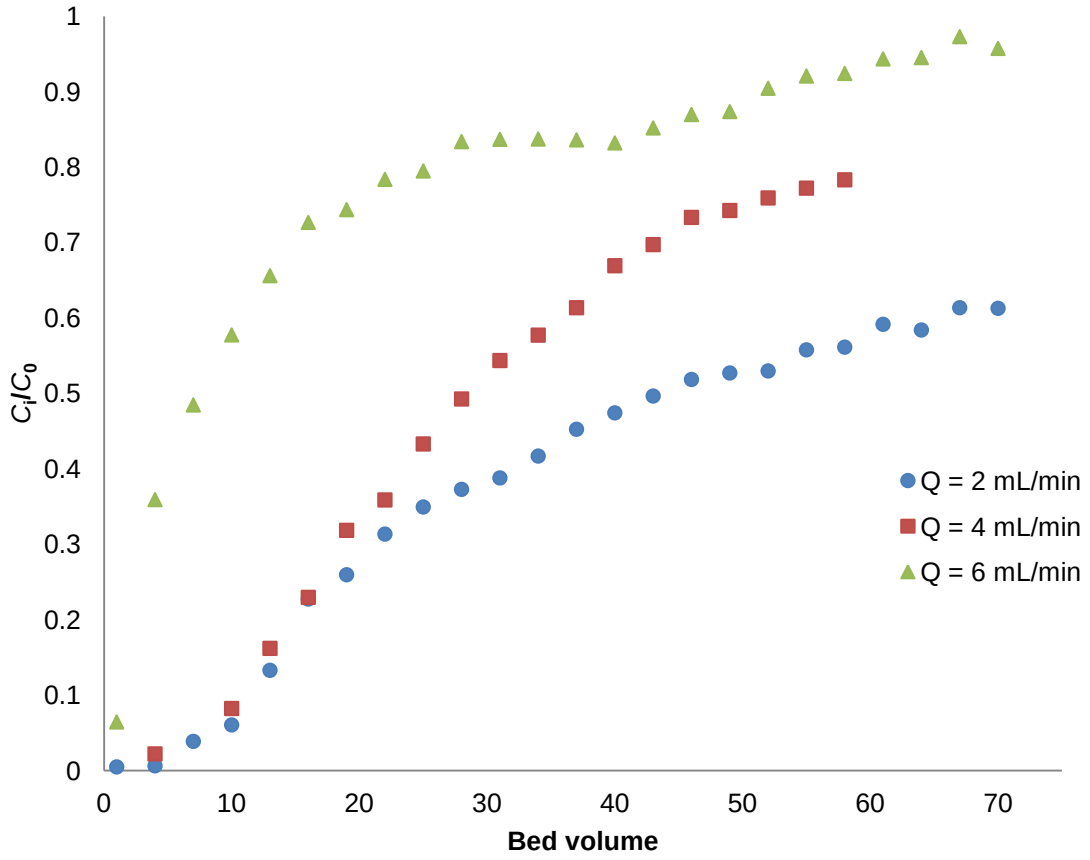

Figure 36. Breakthrough curve of phosphorus on acidified laterite column.
Particle size: 500 µm < Φ < 600 µm; C_0 = 10 ppm; BV = 9 mL; pH = 7.

From the figure above it is clear to see that the shape of the breakthrough curves is not very sharp, in contrast with which was expected from the theory. This may be attributed to a preferential way of the fluent inside the column, and also due to a velocity profile which makes the particles in the middle of the column get saturated before those ones closer to the internal surface of the column.

On the other hand, the breakthrough point can be obtained from Figure 36 considering the ratio C_t/C_0 = 0.1, as outlined in table 15 below:

Table 15. Breakthrough point of laterite column to phosphorus.

Flow rate Q (mL/min)	**Bed volume at C_i/C_0 = 0.1**	**Breakthrough time t_b (min)**
2	11.69	17.53
4	10.55	23.73
6	1.19	5.34

In order to obtain the adsorption capacity of laterite column to phosphate, the following model was applied:

$$X = \frac{\left(t_e - \int_{t_b}^{t_e} f(t)\,dt\right) Q\, C_0}{m} \tag{20}$$

Where:

- X is the adsorption capacity of the column.
- t_b is the time of breakthrough point.
- t_e is the time at exhaustion.
- $\int_{t_b}^{t_e} f(t)\,dt$ is the area under the breakthrough curve.

It may be noted here that the time at exhaustion can only be considered for the highest flow rate (Q_3 = 6 mL/min), since it is the only case in which exhaustion was reached with the obtained experimental data (see Figure 36). Therefore, the time at exhaustion was considered as the time at BV = 58, in order to get a logical comparison between the three flow rates, although the adsorption capacity for the highest flow rate can be considered very similar to that one which would be obtained with the real value of exhaustion time. The results of adsorption capacities are presented in Table 16 below:

Table 16. Adsorption capacities of laterite column to phosphorus.

Flow rate *Q* (mL/min)	***X* (mg P / g laterite)**
2	0.951
4	0.794
6	0.369

The highest adsorption capacity was obtained with the lowest flow rate, as expected from Figure 36, since it graphically corresponds to the area above the breakthrough curve. Nevertheless, it is necessary to point out that the results are much lower than those obtained from the batch experiments. This is due to the fact that a true equilibrium is never attained in this kind of dynamic processes, since the contact time in column system is limited –it can be calculated as the residence time in the column–, and it will always be lower than the time needed to reach true equilibrium, as showed in section 4.3 (Adsorption Kinetics).

5. Result Comparison

5.1. Comparison with Other Materials

Some other isotherm studies were also carried out, but using synthetic iron oxides as an adsorbent instead of laterite. These iron oxides possessing high surface area (273.31 m^2/g) were produced using $Fe(NO_3)_3 \cdot 9\,H_2O$ as the iron source, Pluronic P-123 ($PEO_{20}PPO_{70}PEO_{20}$) as a surfactant and ammonium hydroxide as a precipitation agent. The sample tested was produced as follow: 1 g of P-123 was dissolved in 100 mL of Fe^{3+} solution respecting a molar ratio of 250 for Fe^{3+}/P-123. The solution was steered during 2 hours until a cleared solution was obtained. The pH was then slowly rose using a 25% NH_3OH solution and stirred further for 1 hour. The glass flask was closed and the solution allowed to age at 60 °C for 16 hours. The precipitated was then filtered and cleaned with deionised water to remove any excess of P-123 and dried at 60 °C. The dried material was soaked in methanol at 60 °C and shacked overnight to remove incorporated surfactant. Finally the powder produced was filter and dried at 60 °C.

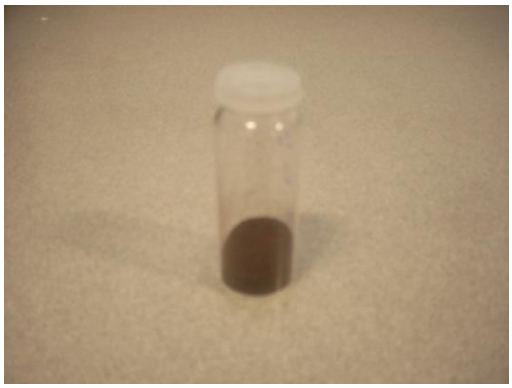

Figure 37. Sample of synthetic iron oxides.

The rest of conditions were exactly the same as described in section 4.4.1. This was made in order to see the efficiency of laterite compared to other materials commonly used in adsorption processes, such as iron oxides.

The results obtained from these adsorption isotherm experiments are outlined in Figures 38 and 39:

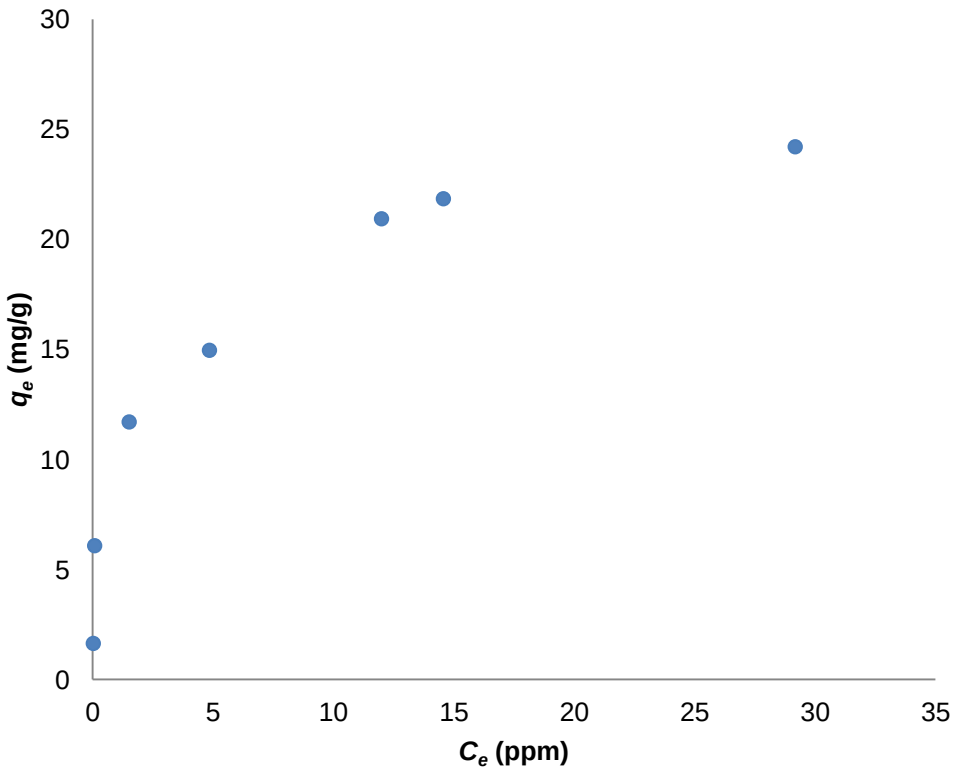

Figure 38. Phosphorus adsorption isotherm for synthetic iron oxides.
Particle size: Φ < 75 µm; temperature = 25 ºC; adsorbent dose = 1 g/L; pH = 7.

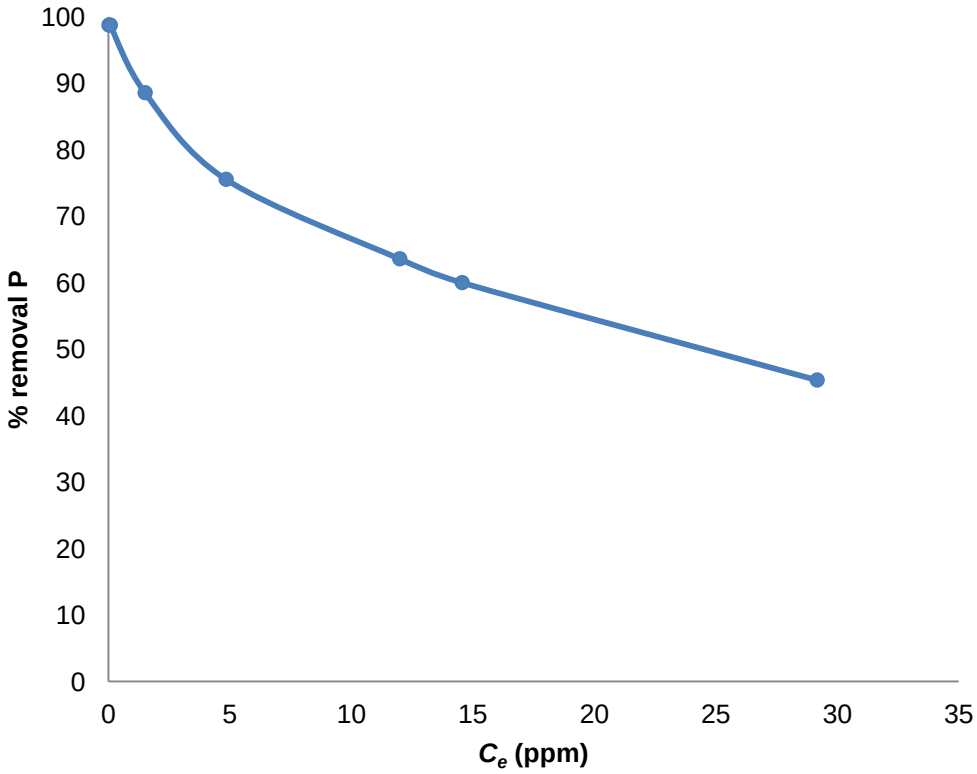

Figure 39. Percentage of removal of P for synthetic iron oxides.
Particle size: Φ < 75 µm; temperature = 25 ºC; adsorbent dose = 1 g/L; pH = 7.

The results are clearly much better than those obtained with the acidified laterite, as the maximum adsorption capacity is now approximately 24.21 mg/g, while in section 4.4.1 the value of this same parameter was 2.75 mg/g. Therefore, this new value is almost 9 times the maximum adsorption capacity of acidified laterite. This change is probably related to the surface area of the new material, which is also much higher than that one from the acidified laterite.

A higher efficiency for P adsorption into iron oxide is also shown in Figure 39, as the percentage of removal of phosphorus found with the lowest equilibrium concentration is approximately 99%, in contrast with the 44% obtained with acidified laterite for the same experimental conditions.

As done in section 4.4.2, the experimental data were fitted to both Freundlich and Langmuir equations, in order to find a suitable model for the phosphorus adsorption onto synthetic iron oxides. The estimated values of adsorption parameters obtained from these models are shown in Table 17:

Table 17. Freundlich and Langmuir adsorption constants for P sorption on synthetic iron oxides.

Freundlich model			**Langmuir model**		
K_F	n	R^2	K_L (L/mg)	Q_0 (mg/g)	R^2
9.048	3.004	0.926	0.698	24.691	0.990

The experimental data fitted well the Freundlich and Langmuir equations, with correlation coefficients ranging from 0.926 to 0.990 (~1). On the other hand, only the Q_0 value from the Langmuir model is reliable, as it is very similar to the maximum adsorption capacity obtained with the experimental data (24.21 mg/g). Therefore, the Langmuir model was applied in order to obtain a mathematical model for the adsorption process. The equation that can be applied to the adsorption process of phosphate onto synthetic iron oxides is based in the following equation:

$$q_e = \frac{17.241 C_e}{1 + 0.698 C_e} \tag{21}$$

Finally, a graph with both experimental and Langmuir model data was made in order to confirm the similarity between the experimental and the mathematical model, as shown in Figure 40:

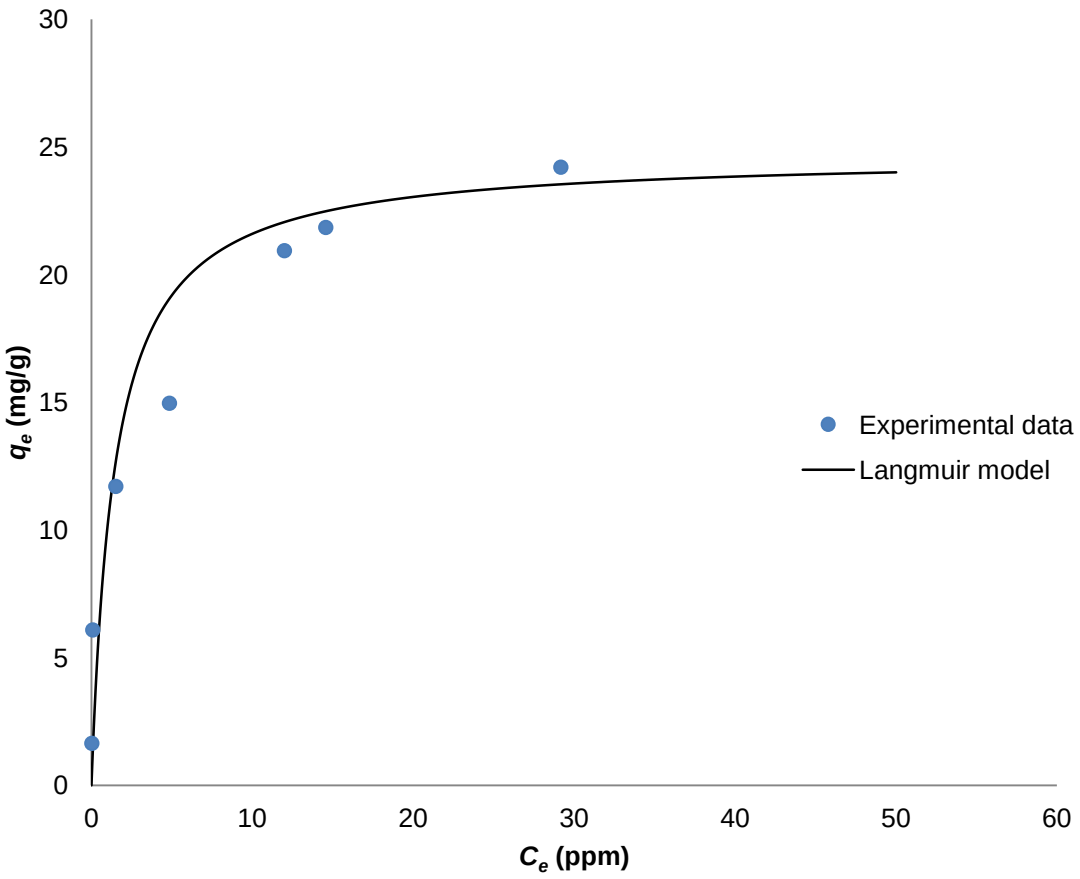

Figure 40. Comparison between experimental and Langmuir model data for P adsorption on synthetic iron oxide (particle size: Φ < 75 µm). Temp. = 25 ºC; adsorbent dose = 1 g/L; pH = 7.

From the above figure, it can be concluded that the Langmuir model fits with the experimental data in terms of shape, with only some deviations for the medium concentration data within the working range. Even so, both models present more differences between them than those in section 4.4.2 (model for acidified laterite), due to a lower correlation coefficient (R^2) in this last case.

5.2. Comparison with Other Authors

In order to compare the efficiency of the acidified laterite with some other adsorbents regarding phosphorus adsorption, a study based on the literature review about the maximum adsorption capacity in different papers was done. The results of this study are outlined in Table 18 below:

Table 18. Comparative table of maximum adsorption capacity q_m for different studies.

Author(s)	Adsorbent	Particle size	Phosphorus concentration range (ppm)	q_m (mg/g)
Zhang et al. (2011)	Natural laterite (Wuhan, China)	590 - 750 nm	0 - 25	1.07
Current study	Acidified laterite (Northern Ireland)	< 75 µm	1 - 50	2.75
Li et al. (2009)	Lanthanum doped vesuvianite (Yunnan, China)	-	0 - 4	6.70
Zeng et al. (2003)	Iron oxide tailings (Alberta, Canada)	68.6 µm (average)	0 - 20	8.21
Xiong and Mahmood (2010)	Peat (Jilin, China)	< 1 mm	0 - 120	8.91
Xu et al. (2010)	Modified fly ash (Eastern China)	< 50 µm	0 - 20	9.15
Current study	Synthetic iron oxides (Northern Ireland)	< 75 µm	1 - 50	24.21
Liu et al. (2007)	Active red mud (Shandong, China)	10 mesh (2 mm)	1 - 2500	95.86
Özacar, M. (2002)	Alunite (Şaphane, Turkey)	90 - 150 µm	5 - 200	118

From the above table it can be concluded that the acidified laterite used in the current study is clearly far from other adsorbents in terms of adsorption capacity, although it is still better than natural laterite, as previously suggested in the Adsorption Kinetics (see section 4.3). Even so, red mud and alunite can be considered the best adsorbents for phosphorus, as their maximum adsorption capacity is more than 10 times higher than those from the other studied adsorbents.

6. Conclusions and Perspectives

Based on results of this work, it can be concluded that the laterite is an interesting option for removing phosphate from fresh or waste water, although it is clear that the adsorption process has some limitations.

Modification of laterite by acid significantly enhances its phosphate immobilization ability; although the time needed to reach equilibrium will be approximately 8 hours in any case. The adsorption kinetics of phosphorus on acidified laterite can be well described by a pseudo-second-order model.

The Langmuir isotherm was found to be the best mathematical model to describe the adsorption isotherms of phosphorus removal onto acidified laterite. The adsorption process can be considered favourable in terms of affinity of the adsorbent for the solute within the working range of initial phosphorus concentration.

An increasing in the temperature of the process results in a higher adsorption capacity, suggesting an endothermic process. This was confirmed by the determination of the thermodynamic parameters, which also showed the spontaneous nature of adsorption.

High percentages of removal –close to 100%– can be reached with adsorbent dosages above 8 g/L for an initial phosphorus concentration of 25 ppm, with final phosphorus concentrations that satisfy the EC UWWT Directive in most of the cases.

Among the parameters studied, pH is proved to be the key variable for phosphate uptake. The results show that the process is more effective in the highly acid pH region –between pH 3 and 5–, due to a point of zero charge of the laterite near to pH 5. These results also suggest that the phosphorus adsorptive process onto acidified laterite is based on chemisorption and electrostatic interactions.

The column adsorption experiments suggest that phosphate in industrial wastewater could be removed as efficiently as in batch experiments for sufficiently low flow rates. This would simulate the conditions of batch experiments as long as the contact time inside the column is similar to the one needed to reach a true equilibrium.

Finally, it is necessary to point out that regardless of its local availability; laterite is still far from other adsorbents in terms of adsorption capacity. Therefore, it would be interesting for future research to repeat similar experiments with other synthetic adsorbents, such as iron oxides, which showed much higher adsorption capacity than most of the adsorbents from literature.

7. References

- Albadarin, A. B.; Mangwandi, C.; Al-Muhtaseb, A. H.; Walker, G. M.; Allen, S. J.; Ahmad, M. N. M. Kinetic and thermodynamics of chromium ions adsorption onto low-cost dolomite adsorbent. *Chemical Engineering Journal* 2012, *179*, 193–202.
- Al-Ghouti, M. A.; Li, J.; Salamh, Y.; Al-Laqtah, N.; Walker, G.; Ahmad, M. N. M. Adsorption mechanisms of removing heavy metals and dyes from aqueous solution using date pits solid adsorbent. *Journal of Hazardous Materials* 2010, *176*, 510–520.
- Awual, M. R.; Jyo, A.; Ihara, T.; Seko, N.; Tamada, M.; Lim, K. T. Enhanced trace phosphate removal from water by zirconium(IV) loaded fibrous adsorbent. *Water Research* 2011, *45*, 4592–4600.
- Demirbas, E.; Kobya, M.; Senturk, E.; Ozkan, T. Adsorption kinetics for the removal of chromium(VI) from aqueous solutions on the activated carbons prepared from agricultural wastes. *Water S. A.* 2004, *30*, 533–540.
- Gibbons, M. K.; Gagnon, G. A. Understanding removal of phosphate or arsenate onto water treatment residual solids. *Journal of Hazardous Materials* 2011, *186*, 1916–1923.
- Huang, X.; Liao, X.; Shi, B. Adsorption removal of phosphate in industrial wastewater by using metal-loaded skin split waste. *Journal of Hazardous Materials* 2009, *166*, 1261–1265.
- Karageorgiou, K.; Paschalis, M.; Anastassakis, G. N. Removal of phosphate species from solution by adsorption onto calcite used as natural adsorbent. *Journal of Hazardous Materials* 2007, *139*, 447–452.
- Li, H.; Ru, J.; Yin, W.; Liu, X.; Wang, J.; Zhang, W. Removal of phosphate from polluted water by lanthanum doped vesuvianite. *Journal of Hazardous Materials* 2009, *168*, 326–330.
- Liu, H.; Sun, X.; Yin, C.; Hu, C. Removal of phosphate by mesoporous ZrO_2. *Journal of Hazardous Materials* 2008, *151*, 616–622.
- LIU, C.; LI, Y.; LUAN, Z.; CHEN, Z.; ZHANG, Z.; JIA, Z. Adsorption removal of phosphate from aqueous solution by active red mud. *Journal of Environmental Sciences* 2007, *19*, 1166–1170.
- Lu, S. G.; Bai, S. Q.; Zhu, L.; Shan, H. D. Removal mechanism of phosphate from aqueous solution by fly ash. *Journal of Hazardous Materials* 2009, *161*, 95–101.
- Maiti, A.; Basu, J. K.; De, S. Experimental and kinetic modeling of As(V) and As(III) adsorption on treated laterite using synthetic and contaminated groundwater: Effects of phosphate, silicate and carbonate ions. *Chemical Engineering Journal*.

- Maiti, A.; DasGupta, S.; Basu, J. K.; De, S. Adsorption of arsenite using natural laterite as adsorbent. *Separation and Purification Technology* 2007, *55*, 350–359.
- Murphy, J.; Riley, J. P. A Single-Solution Method for the Determination of Soluble Phosphate in Sea Water. *Journal of the Marine Biological Association of the United Kingdom* 1958, *37*, 9–14.
- Özacar, M. Adsorption of phosphate from aqueous solution onto alunite. *Chemosphere* 2003, *51*, 321–327.
- Salameh, Y.; Al-Lagtah, N.; Ahmad, M. N. M.; Allen, S. J.; Walker, G. M. Kinetic and thermodynamic investigations on arsenic adsorption onto dolomitic sorbents. *Chemical Engineering Journal* 2010, *160*, 440–446.
- Seida, Y.; Nakano, Y. Removal of phosphate by layered double hydroxides containing iron. *Water Research* 2002, *36*, 1306–1312.
- Tian, S.; Jiang, P.; Ning, P.; Su, Y. Enhanced adsorption removal of phosphate from water by mixed lanthanum/aluminum pillared montmorillonite. *Chemical Engineering Journal* 2009, *151*, 141–148.
- Tsang, S.; Phu, F.; Baum, M. M.; Poskrebyshev, G. A. Determination of phosphate/arsenate by a modified molybdenum blue method and reduction of arsenate by $S_2O_4^{2-}$. *Talanta* 2007, *71*, 1560–1568.
- Wood, R.; McAtamney, C. Constructed wetlands for waste water treatment: the use of laterite in the bed medium in phosphorus and heavy metal removal. *Hydrobiologia* 1996, *340*, 323–331.
- Xiong, J. B.; Mahmood, Q. Adsorptive removal of phosphate from aqueous media by peat. *Desalination* 2010, *259*, 59–64.
- Xu, K.; Deng, T.; Liu, J.; Peng, W. Study on the phosphate removal from aqueous solution using modified fly ash. *Fuel* 2010, *89*, 3668–3674.
- Zeng, L.; Li, X.; Liu, J. Adsorptive removal of phosphate from aqueous solutions using iron oxide tailings. *Water Research* 2004, *38*, 1318–1326.
- Zhang, L.; Hong, S.; He, J.; Gan, F.; Ho, Y. Adsorption characteristic studies of phosphorus onto laterite. *Desalination and Water Treatment* 2011, *25*, 98–105.
- ZHANG, B.; WU, D.; WANG, C.; HE, S.; ZHANG, Z.; KONG, H. Simultaneous removal of ammonium and phosphate by zeolite synthesized from coal fly ash as influenced by acid treatment. *Journal of Environmental Sciences* 2007, *19*, 540–545.

Appendix A. Kinetics, Isotherms and Thermodynamics Data

Table A1. Comparison of the first- and second-order reaction constants for acidified laterite.

First-order kinetic model			Second-order kinetic model		
k_1 (h^{-1})	q_e	R^2	k_2 (g mg^{-1} h^{-1})	q_e	R^2
0.134	0.772	0.843	0.396	2.743	0.999

Table A2. Freundlich and Langmuir adsorption constants for P adsorption on acidified laterite.

Freundlich model			Langmuir model		
K_F	n	R^2	K_L (L/mg)	Q_0 (mg/g)	R^2
2.088	13.550	0.981	0.900	2.793	0.999

Table A3. R_L values for P adsorption on acidified laterite.

C_0 (ppm)	R_L value	Nature of adsorption process
5	0.182	Favourable
10	0.100	Favourable
15	0.069	Favourable
20	0.053	Favourable
25	0.043	Favourable
30	0.036	Favourable
40	0.027	Favourable
50	0.022	Favourable

Table A4. Langmuir constants for P adsorption on acidified laterite at different temperatures.

T (K)	Langmuir model		
	K_L (L/mg)	Q_0 (mg/g)	R^2
298	0.900	2.793	0.999
303	0.749	2.910	0.999
313	0.552	3.109	0.999
323	0.500	3.367	0.999

Table A5. Thermodynamic parameters for P adsorption on acidified laterite.
Particle size: Φ < 75 µm; adsorbent dose = 1 g/L; pH = 7; C_0 = 50 ppm.

***T* (K)**	**Thermodynamic parameters**		
	(ΔH^0) (kJ/mol)	**(ΔS^0) (J mol^{-1} K^{-1})**	**(ΔG^0) (kJ/mol)**
298	5.545	-5.055	-3.836
303			-3.995
313			-4.285
323			-4.631

Table A6. Freundlich and Langmuir adsorption constants for P sorption on synthetic iron oxides.

Freundlich model			**Langmuir model**		
K_F	***n***	**R^2**	***K_L* (L/mg)**	***Q_0* (mg/g)**	**R^2**
9.048	3.004	0.926	0.698	24.691	0.990

Appendix B. COSHH Risk Assessment

QUEEN'S UNIVERSITY BELFAST

COSHH RISK ASSESSMENT

Title: "Phosphates removal using laterite and modified laterite"
Student: Martín Mendez Pasarín
Supervisor: Dr Gavin Walker

Phase 1: Phosphate removal using laterite

1. What is the process/work activity and where will you be carrying it out?

Project

All experiments will be carried out in laboratory OG-410; QUESTOR furnace in OG-009 will be used. The aim of the research is to study the removal capacity of laterite and modified laterite toward phosphate. A calibrate with the colorimetric method for phosphates determination will be carried out. Adsorption experiments planned include: isotherms, kinetics, pH studies and columns studies. Laterite charred at different temperatures will be used; different particles sizes will also be tested.

Chemical used

- The chemical used during experiments are:
  - Potassium dihydrogen phosphate
  - Ascorbic acid
  - Ammonium molybdate
  - Potassium antimonyl tartrate
  - Sulfuric acid
  - Nitric acid
  - Hydrochloric acid
  - Sodium hydroxide
  - Potassium hydroxyde
  - Deionized water

- Raw materials:
  - Laterite (Aluminium, iron and silica oxides minerals)

- The physical process used are:
  - Heating with: heating stirrers, mantle, water bath, oven, furnace
  - Washing and separation with: deionised water, centrifuge
  - Drying with: oven, vacuum drying

Phosphates measurement

Phosphate will be measured using the Hach spectrophotometer (Method called "Modified molybdenum blue"). Calibration curves will be compared with ICP-AES measure from laboratory OG-201.

Specific hazard: Reagents from the "Modified molybdenum blue"

All synthesis reactions will be carried out under a fume cupboard equipped.

2. What hazardous substances will you be using?

Name of Substance(s) used	Hazard Classification*								Nature of health hazard and route of entry into body	OEL (mg/m^3)
	1	2	3	4	5	6	7	8		
I. Potassium dihydrogen phosphate (KH_2PO_4)			X		X				May cause irritation to skin, eyes and respiratory system.	TWA: n/a STEL: n/a
II. Ascorbic acid ($C_6H_8O_6$)		X	X		X				Slightly hazardous in case of skin contact (irritant), of eye contact (irritant), of ingestion, of inhalation.	TWA: n/a STEL: n/a
III. Ammonium molybdate ($(NH_4)_6Mo_7O_{24}\cdot 4H_2O$)		X	X	X					Corrosive. May be harmful if inhaled. May be harmful or fatal if swallowed. Causes severe burns to eyes and skin.	TWA: 5 $mg.m^{-3}$ STEL: 20 $mg.m^{-3}$
IV. Potassium antimonyl tartrate ($C_4H_4O_7SbK$)	X	X	X	X					Harmful if inhaled or swallowed. Toxic to aquatic organisms, may cause long-term adverse effects in the aquatic environment. May cause liver damage.	TWA: 0.5 $mg.m^{-3}$ STEL: n/a
V. Sulfuric acid (H_2SO_4)		X	X	X	X				Causes severe skin burns. Causes severe eye burns. Causes burns of the mouth, throat, and stomach.	TWA: 1 $mg.m^{-3}$ STEL: n/a
VI. Nitric acid (HNO_3)		X	X	X					Strong oxidizer. Contact with other material may cause fire. Corrosive. Liquid and mist cause severe burns to all body tissue. May be fatal if swallowed or inhaled. Inhalation may cause lung and tooth damage.	TWA: 5.2 $mg.m^{-3}$ STEL: 10 $mg.m^{-3}$
VII. Hydrochloric acid (HCl)		X	X	X					Corrosive. Liquid and mist cause severe burns to all body tissue. May be fatal if swallowed or inhaled.	TWA: 2 $mg.m^{-3}$ STEL: 8 $mg.m^{-3}$
VIII. Sodium hydroxide (NaOH)		X	X	X					Corrosive. Liquid and mist cause severe burns to all body tissue. May be fatal if swallowed or inhaled.	TWA: 2 $mg.m^{-3}$ STEL: 10 $mg.m^{-3}$
IX. Potassium hydroxide (KOH)			X	X					Corrosive. May cause serious burns. Harmful by ingestion, inhalation and in contact with skin. If the solid or solution comes into contact with the eyes, serious eye damage may result.	TWA: n/a STEL: 2 $mg.m^{-3}$
X. Deionized water										

*** 1. Very Toxic 2. Toxic 3. Harmful 4. Corrosive 5. Irritant 6. Respiratory Sensitiser**
7. Carcinogen, mutagen or teratogen (agent toxic to reproduction) 8. Micro-organism/Biological Agent

STEL: Short Term Exposure Limit (15 min)
TWA: Time weighted average (over 8 hours)

3. How long will the process/work activity last? What will the exposure pattern be?

Phosphate measurement method time is in the order of minutes.

Kinetics adsorption studies are in the order of hours.

4. Can you prevent exposure to the hazardous substances?

~~By doing any of the following?:~~

~~(a) using a different process; or~~
~~(b) using alternative substances; or~~
~~(c) using different forms of the same substance~~

~~If YES, to any of the above repeat Sections 1 – 4 again and proceed to Section 5.~~

If NO, continue into next section.

5. Which precautionary measures will you be using for the work process/activity? (Tick as appropriate)

		X			
Total Containment	Partial Containment	LEV	Dilution Ventilation	PPE	Other (please state)

6. Which type of personal protective equipment will you be using? (if required)

		X	**X**		
Respiratory	Face	Eye	Hand	Foot	Other (Aprons etc) (please state)

7. Who is likely to be exposed to the hazardous substances that you will be working with?

Me and potentially other workers at the laboratory OG-410 and OG-009.

8. Is a "permit-to-work" required to prevent exposure to others? NO

9. Is air monitoring required? NO

10. Is health surveillance required? NO

11. What are the procedures for dealing with unplanned releases and spillages?

I. Ventilate area of leak or spill. Wear appropriate personal protective equipment. Vacuum or sweep up. Vacuuming or wet sweeping materials should avoid dust dispersal and be disposed as hazardous material.

II - III. Use appropriate tools to put the spilled solid in a convenient waste disposal container. Finish cleaning by spreading water on the contaminated surface.

IV. Dilute with water and mop up, or absorb with an inert dry material and place in an appropriate waste disposal container. Finish cleaning by spreading water on the contaminated surface.

V - X. Neutralize material (with soda ash or lime or acid), then absorb with an inert material (vermiculite, dry sand, earth). Ventilate area of leak or spill. Place in a chemical waste container the adsorbent materials. Do not get water on spilled substances or inside containers. Use appropriate personal protective equipment.

12. What are the procedures for disposing of the hazardous substances?

I. Residual water from experiments can be evacuated by the sink when low phosphate concentration is present. High concentrated solution can be treated by precipitation and disposal of the solid part into the laboratory bin.

II - IV. Waste should be collected in a suitable lidded waste container clearly labelled as Toxic, Irritant and/or corrosive. It has to be disposed of using the Scholl Waste Chemical Disposal Procedure.

V - X. Solution having a low concentration of acid or base can be evacuated into the sink. Concentrated solution can be neutralize with opposite.

13. What training is required for the work process/activity?

- No training required.

*** (delete as appropriate)**

14. Conclusions

It is considered that the quantities, rates and manner of use of the substances detailed in this risk assessment, do not constitute any significant risk to health when the control measures indicated:

- are working
- are maintained in good working order
- and are used in accordance with training given

Signed: Project Worker _____ Date _____

_____ _____

_____ _____

_____ _____

_____ _____

_____ _____

_____ _____

_____ _____

_____ _____

_____ _____

_____ _____

Signed: Project Supervisor _____ Date _____

Signed: COSHH Supervisor _____ Date _____

Review Date _____

September 2011